EFFECT OF SOFT SEGMENT STRUCTURE AND HARD SEGMENT CONTENT ON THE SURFACE AND BULK PROPERTIES OF SEGMENTED POLYURETHANEUREAS

by

Melis Peniç

A Thesis Submitted to the

Graduate School of Sciences and Engineering

In Partial Fulfillment of the Requirements for the

Degree of

Master of Science in

Biomedical Sciences and Engineering Program

Koç University

September 2014

Koç University

Graduate School of Sciences and Engineering

This is to certify that I have examined and this copy of the master's thesis written by

Melis Peniç

And have found that it is complete and satisfactory in all aspects,

And that any and all revisions required by the final

examining committee have been made.

Committee members:

_____

Prof. Dr. İskender Yilgor (Advisor)

_____

Prof. Dr. Yusuf Menceloğlu

_____

Assoc. Prof. Dr. Funda Yağcı Acar

Date: 30/09/2014

ABSTRACT

Due to their interesting combination of bulk and surface properties segmented thermoplastic polyurethanes (TPU), polyureas and polyurethaneureas (TPUU) find wide range of applications in many diverse fields. One of the emerging applications of TPUUs include their usage as biomaterials in blood contacting applications. This is mainly due to the possibility of designing and synthesizing TPUUs with controlled bulk and surface properties that possess very good blood and tissue compatibility. [1]

The main goals of this study were the investigation of the influence of; (i) soft segment (SS) structure, (ii) SS molecular weight and (iii) hard segment (HS) content on the morphology and bulk and surface properties of TPUUs. In addition, another aim was to investigate the relationship between the surface energies of copolymers and their resistance to biofilm formation.

A large number of segmented thermoplastic poly(urethaneurea)s (TPUU), polyurethanes (TPU) and polyureas (PU) based on five different SS were synthesized by using the conventional two step "prepolymer" polymerization method (or in one step if the polymer was *non-chain extended*) and characterized. Bis(4-isocyanatocyclohexyl)methane (HMDI) was used as the diisocyanate and 2-methyl-1,5-diaminopentane (MDAP) or 1,4 butanediol (BD) was used as the chain extender. Five different SS which were used in this study included poly(ethylene oxide) glycol (PEO), poly(propylene oxide) glycol (PPO), poly(tetramethylene oxide) glycol (PTMO), aminopropyl and hydroxyhexyl terminated polydimethylsiloxane (PDMS) and a hydroxy terminated polyfluoroether (PFE) oligomer (Fluorolink E10-H®). HS contents of the copolymers were generally kept constant at 20 and 30% by weight with a few exception. To investigate the influence of the molecular weight, SS oligomers with two different molecular weights of 1,000 and 2,000 g/mol were used during the synthesis.

The bulk and surface properties of all polymers were characterized by using a large number of techniques, which included; ATR-FTIR (Attenuated Total Reflection Fourier Transform Infrared), DSC (Differential Scanning Calorimetry), SAXS (Small Angle X-ray Scattering) and stress strain analysis, AFM (Atomic Force Microscopy), XPS (X-ray Photoelectron Spectroscopy) and static water contact angle measurements.

Selected copolymers with different surface energies were also tested for biofilm formation. Results obtained indicated extensive biofilm formation on all samples regardless of their surface properties.

Characterization results showed that polyether based copolymers, especially those with PEO SS, displayed poor microphase separation when compared with PDMS and PFE based copolymers. This is expected since the polyethers used in this study have higher solubility parameters and ether groups can form hydrogen bonding with urethane and urea groups, which is not possible in case of PDMS and PFE. Surface characterization by contact angle measurements showed dramatic differences depending on the SS structure and molecular weight. As indicated by XPS studies, in general the soft segments tend to migrate to the polymer surface and affect the hydrophobicity and hydrophilicity of the copolymer depending on their solubility parameters.

The extent of biofilm formation was not affected by the surface energy differences within the copolymers. Many alternatives for the bacterium sticking mechanism on surfaces have been proposed in the literature. [2] Some studies suggest that bacterium tend to stick on hydrophilic surfaces[3], while other studies suggest that bacterium tend to stick on hydrophobic surfaces [2]. It should also be noted that the sticking mechanism of every strain of bacterium is different [4], which makes this concept even more challenging to explain. Therefore our study is a contribution to the literature on this topic and suggests that the sticking mechanism of *Staphylococcus aureus* 700698 strain of bacterium is not affected by the surface of the polymer being hydrophilic or hydrophobic.

ÖZET

Çok kısımlı termoplastik poliüretanlar, poliüreler ve poli(üretanüre)ler (TPU) yığın ve yüzey özelliklerinin ilginç kombinasyonu sayesinde bir çok sektörde geniş uygulama alanları bulurlar. Biyomedikal alanı, termoplastik poli(üretanüre)lerin son zamanlarda özellikle kan temas uygulamaları için kullanılmaktadır. TPU'ların biyomedikal malzeme olarak geniş kullanım bulmalarının nedeni, kan ve doku uyumunu sağlayacak yığın ve yüzey özelliklerini elde edebilmek adına kontrollü bir şekilde tasarlanabilir ve sentezlenebilir olmalarıdır. [1]

Bu çalışmanın ana amacı biyomedikal uygulamalar için tasarlayıp sentezlediğimiz TPU'larda (i) yumuşak kısım yapısının, (ii) yumuşak kısım moleküler ağırlığının ve (iii) sert kısım miktarının bu kopolimerlerin morfoloji, yığın ve yüzey özelliklerine yaptığı etkileri araştırmaktır. Buna ek olarak, kopolimerlerin yüzey enerjileri ile üzerlerinde büyüyen biyofilmlere karşı olan dirençleri arasındaki ilişkiyi araştırmaktır.

Bu amaçla bu tez çalışmasında genel olarak iki aşamalı bir sentez yöntemi (prepolimer yöntemi) kullanılarak beş farklı yumuşak kısımdan oluşan çok sayıda termoplastik poli(üretanüre), poliüretan ve poliüre kopolimerleri sentezlenmiş ve karakterize edilmiştir. Sert kısımlar, halkalı alifatik bis(4-izosiyanatosiklohekzil)metan (HMDI) ve zincir uzatıcı olarak 2-metil-1,5-diaminopentan (MDAP) veya 1,4-bütandiol (BD) kullanılarak oluşturulmuştur. Yumuşak kısımlar ise polietilen glikol (PEO), polipropilen glikol (PPO), politetrametilen glikol (PTMO), aminopropil veya hidroksialkil uçlu polidimetilsiloksan (PDMS) ve hidroksil uçlu poliflorüreter (PFE) (E10-H®) oligomerleri kullanılarak oluşturulmuştur. Birkaç istisna dışında, sert kısımlar ağırlıkça %20 ve %30 olarak sabit tutulmuştur. Yumuşak kısımların moleküler ağırlıklarının polimer üzerindeki etkisini araştırmak için sentez esnasında ortalama molekül ağırlıkları 1.000 ve 2.000 g/mol olan oligomerler kullanılmıştır.

Yığın ve yüzey özelliklerini belirlemek amacıyla bütün kopolimerler FTIR (Fourier Transform Kızılötesi Spektroskopisi), DSC (Diferansiyel Taramalı Kalorimetri), SAXS (Düşük açılı X-Işınları Saçılımı), AFM (Atomik Kuvvet Mikroskopisi), XPS (X-Işınları Fotoelektron Spektroskopisi), çekme-kopma deneyleri ve suyun polimer yüzeyi ile yaptığı kontak açısı ölçümleri ile karakterize edilmişlerdir. Yüzey enerjilerinde farklılık gösteren polimerler seçilmiş ve üzerlerinde biyofilm oluşum testleri yapılmıştır. Yüzey özelliklerinin farklılık göstermelerine rağmen bütün polimerde yoğun oranda biyofilm oluşması gözlemlenmiştir.

Karakterizasyon sonuçları, polieter bazlı polimerlerde ve özellikle de PEO bazlı polimerlerde, PDMS ve PFE bazlı kopolimerlerle karşılaştırıldıkları zaman, zayıf oranda mikrofaz ayrımı olduğunu gösterdi. Bu çalışmada kullanılan polieterlerin çözünürlük parametrelerinin yüksek olmalarından ve PDMS ve PFE'lerden farklı olarak eter gruplarının üretan ve üre grupları ile hidrojen bağı yapabilmelerinden ötürü bu beklenen bir sonuçtu. Kontak açısı ölçümleri, yumuşak kısmın kimyasal farklılığına ve ortalama molekül ağırlıklarına bağlı olarak polimerlerin yüzey özelliklerinin oldukça farklı gösterdiğini kanıtlamıştır. XPS çalışmaları ise yumuşak kısımların genel olarak yüzeyde toplandığını ve çözünürlük parametrelerine göre kopolimer yüzeylerine hidrofobik veya hidrofilik özellik verdiğini göstermiştir.

Yüzeydeki enerji farklılıklarının kopolimer yüzeyindeki biyofilm oluşma derecesini etkilemediği gözlemlenmiştir. Literatürde bakterilerin yüzeye tutunma mekanizmaları hakkında bir çok alternatif bulunmaktadır [2]. Bazı çalışmalar bakterilerin hidrofilik yüzeylere daha rahat tutunduklarını gösterirken [3], bazı çalışmalar ise bakterilerin hidrofobik yüzeylere daha rahat tutunduklarını göstermektedir [2]. Ayrıca her bakteri türünün yüzeye tutunma mekanizmasının farklı olması da, bu konsepti açıklamayı daha karmaşık hale getirir. [4] Bu çalışmamız literatüre bu konuda bir katkı sağlayacak niteliktedir ve *Staphylococcus aureus* 700698 bakteri türünün yüzeye tutunma mekanizmasının yüzeyin hidrofobik ya da hidrofilik olmasına göre değişim göstermediğini önerir.

ACKNOWLEDGEMENTS

I would like to express my deepest gratitude to those who made this thesis possible and supported me throughout the process. I would like to start by thanking Prof. İskender Yılgör and Emel Yılgör for their endless support, patience and guidance. With this master's thesis I have not only gained academic skills but also have gained working principles that will stay with me for the rest of my life. Some of those principles are; hard working, discipline, cleanliness, organization, honesty and compassion. I have learned these skills because my advisors practice them and encourage us to always become better in what we do. I can definitely say that this has been a life changing experience for me.

I would like to thank Dr. Barış Yağcı and Cansu Yldırım from KUYTAM and Dr. Uğur Ünal for helping me in my experiments throughout my research.

I would like to thank my beloved parents for caring and nourishing me since birth. Without their vision for me to have a good education, I would not have come to this point. They have always supported me in whatever I want to do in my life and I'm sure they will carry on doing so. There are no words to express my gratitude towards them so I will leave it with this. I would also like to thank my brothers Samir Peniç and Kerem Peniç for being awesome brothers.

One big thank you goes to the students of the Polymer Science Lab. Our senior PhD student Çagla Koşak Söz has guided me in all my academic work and has always believed in me even at times when I didn't believe in myself. I can say that she wasn't doing this just for support, she sincerely believed in me, and that was a huge part that got me through my master's thesis. She is a very hard working strong woman with a delicate heart. Armen Yıldırım at times has been like my younger brother and at times has been like my elder brother. I wish him the best in life, and I would officially like to request that he doesn't forget me once he is awarded with the Nobel Prize. Our labs younger PhD student Özgün Önder is one of the most sincere people I have met in my life. His transparency in character has inspired all of us and his jokes have made us laugh for hours at times.

Last but not least I want to thank Dr. Atlığ for always supporting me when I needed; he is family for me; Zeynep Kaya for simply being a beautiful person and Caner Gümüş for the magic he has brought to my life.

TABLE OF CONTENTS

LIST OF TABLES x
LIST OF FIGURES xi
NOMENCLATURE xiii
CHAPTER 1 1
INTRODUCTION 1
1.1 Classification of Polymers 1
1.2. Thermoplastic Elastomers 6
1.3. STPUU synthesis 7
1.4. Structure-Morphology-Property Relations in Segmented PUUs 8
1.5. Factors Affecting the Microphase Separation in Segmented PUUs 9
1.5.1. Chemical Structure of the Soft Segments 10
1.5.2. Effect of Soft Segment Molecular Weight 12
1.5.3. Effect of the Hard Segment Content and Symmetry 13
1.5.4. Hydrogen Bonding 16
1.5. Biomedical Applications of Thermoplastic PUUs 19
1.6. Biofilm formation on polymer surfaces and studies on their inhibition 20
1.7. Purpose of the Study 21
CHAPTER 2 23
EXPERIMENTAL 23
2.1. Materials 23
2.2. Polymer Design and Calculations Used for Determining the Reaction Stoichiometry 25
2.3. Description of the General Reaction Procedure Used for the Preparation of SPUU Copolymers 26
2.3.1. Synthesis of PEO based PUUs 27
2.3.2. Synthesis of PPO based PUUs 28
2.3.3. Synthesis of PTMO Based PUUs 28
2.3.4. Synthesis of PDMS Based PU and TPUs 29
2.3.5. Synthesis of PFE Based PUUs 29
2.3.6. Nomenclature System for the Copolymers Synthesized 30
2.4. Characterization Methods 31
2.4.1. Spectroscopic Analysis 31
2.4.2. Stress-Strain Tests 31

2.4.3. Atomic Force Microscopy 31
2.4.4. Small Angle X-ray Scattering 32
2.4.5. Differential Scanning Calorimetry (DSC) 32
2.4.6. X-Ray Photoelectron Spectrometry (XPS) 33
2.4.7. Static Water Contact Angle Measurements 33
2.5. Biofilm Assays 33
2.5.1. Materials 34
2.5.2. Procedure 34
CHAPTER3 35
RESULTS AND DISCUSSIONS 35
3.1 Structural design and synthesis of PUUs 35
3.2.1. ATR-FTIR Analysis of the Hydrogen Bonding in the Carbonyl Groups 38
3.3. DSC Analysis 47
3.4. Small Angle X-ray Scattering (SAXS) studies 53
3.5. Stress-Strain Analysis 57
3.6. Surface Characterization 59
3.6.1 Atomic Force Microscopy 59
3.7. X-ray Photoelectron Spectrometer (XPS) 62
3.8. Static Water Contact Angle Measurements 65
3.9. Biofilm Assays 66
CHAPTER 4 68
CONCLUSIONS 68
BIBLIOGRAPHY 70
VITA 74

LIST OF TABLES

Table1.1. Solubility parameters of selected soft and hard segments 9

Table1.2. Effect of hydrogen bonding on the tensile properties of segmented polyamides with crystalline HS 18

Table2.1. Chemical structures of the reactants 23

Table2.2. Chemical compositions of the segmented polyurethane, PU and PUU copolymers synthesized in this study 30

Table3.1. Characteristic IR Absorption Frequencies of TPU and PU 38

Table3.2. Summary of DSC data 53

Table3.3. Calculated interdomain spacings (*d*) of copolymers 55

Table3.4. Tensile properties of copolymers 58

Table 3.5. Percent atomic composition of the starting materials used during the preparation of TPUU copolymers 62

Table3.6. Percent Bulk Atomic Compositions of the Copolymers 63

Table3.7. Percent Atomic Compositions of Copolymers obtained from XPS analysis 64

Table3.8. Experimental average water contact angles for PUU copolymers 65

Table3.9. The colony counts of polymers with varying surface energies 67

LIST OF FIGURES

Figure1.1. Classification of polymers based on their macromolecular architecture, chain structure or topology. a) Linear polymer chains. b) Branched polymer chain. c) Cross-linked polymer chains 1

Figure1.2. Stress–strain plots for a typical elastomer, flexible plastic, rigid plastic, and fiber. 2

Figure1.3. The classification polymers depending on the arrangement of monomers 3

Figure1.4. Schematic representation of block copolymers 3

Figure1.5. Schematic representation of alternating soft and hard segments in segmented block copolymers 4

Figure1.6. The formation of urethane and urea linkages 5

Figure1.7. Microphase separation of HS and SS. The darker and thicker blocks are the HS, while the loose matrix is the SS. The HS are stuck together with hydrogen bonding 6

Figure1.8. Two step pre-polymer method for the synthesis of TPUU and representation of SS and HS within the polymer 7

Figure1.9. Schematic representation of the structure-morphology-property relations in segmented TPUUs 8

Figure1.10. DMA behavior of TPU based on PCL, various diisocyanates chain extended with BD containing 20% by weight HS 14

Figure1.11. AFM images of *non chain extended* TPUs based on PTMO1K and corresponding diisocyanates 15

Figure1.12. AFM phase images of *non chain extended* PUs based on PTMO1K and corresponding diisocyanates 16

Figure1.13. Monodentate and bidentate hydrogen bonding between urethane, urea and ether groups 17

Figure1.14. Influence of level of N-substitution on the modulus of polyamide-6,10s 19

Figure3.1. FT-IR spectra of various steps of PTMO2-UU-30 synthesis 37

Figure3.2. ATR-FTIR spectra of polymers with soft segments of 1K and 1.4 K average molecular weights with 16, 20 and 25 % wt hard segments 39

Figure3.3. ATR-FTIR spectra of polymers with soft segments of 1K average molecular weights with 30 % wt hard segments 42

Figure3.4. ATR-FTIR spectra of polymers with soft segments of 2K and 2.5K average molecular weights with 20 % wt HS 44

Figure3.5. ATR-FTIR spectra of polymers with soft segments of 2K and 2.5K average molecular weights with 30 % wt HS 45

Figure3.6. DSC thermogram of PEO2-UU-30 47

Figure3.7. DSC thermogram of PEO1-UU-30 48

Figure3.8. DSC thermogram of PTMO1-UU-30 49

Figure3.9. DSC thermogram of PTMO2-UU-20 49

Figure3.10. DSC thermogram of PTMO2-UU-30 50

Figure3.11. DSC thermogram of PPO2-UU-20 50

Figure3.12. DSC thermogram of PPO2-UU-30 51

Figure3.13. DSC thermogram of PFE1.4-Ur-16 51

Figure3.14. DSC thermogram of PFE1.4-UU-20 52

Figure3.15. SAXS intensity profiles of PPO2-UU-30 and PTMO2-UU-30 54

Figure3.16. SAXS intensity profiles of H-PDMS2.5-Ur-30, A-PDMS2.5-U-20 and A-PDMS2.5-U-30 54

Figure3.17. SAXS intensity profiles of PFE1.4-Ur-16 and PFE1.4-UU-20 55

Figure3.18. AFM phase image of *non-chain extended* PTO1K/HMDI PU 59

Figure3.19. AFM phase images of copolymers. a)PEO2-UU-30 b)PPO2-UU-30 c)PTMO2-UU-30 d)A-PDMS2.5-U-30 e)PFE1.4-UU-20 60

Figure3.20. AFM phase image of PTMO2K/HMDI/DETA, 28%wt HS 61

Figure3.21. Microphase morphology of A-PDMS3K/HMDI, 8%wt HS obtained by bead representation using Dissipative Particle Dynamics calculations 62

NOMENCLATURE

$<M_n>$	Number average molecular weight
AFM	Atomic force microscopy
A-PDMS	Aminopropyl terminated polydimethylsiloxane
ATR-FTIR	Attenuated Total Reflection Fourier Transform Infrared Spectroscopy
BD	1,4-butanediol
CHDI	1,4-Cyclohexyl diisocyanate
d	Interdomain spacing
DBTDL	Dibutyltindilaurate
DMA	Dynamic mechanical analysis
DMF	Dimethylformamide
DSC	Differential scanning calorimetry
MDAP	2-methyl-1,5-diaminopentane
EG	Ethylene glycol
FTIR	Fourier Transform Infrared Spectroscopy
HDI	1,6-Hexamethylene diisocyanate
HMDA	1,6-Hexamethylene diamine
HMDI	Bis(4-isocyanatocyclohexyl)methane
H-PDMS	Hydroxyhexyl terminated polydimethylsiloxane
HS	Hard Segment
IPA	Isopropyl alcohol
MDI	Bis(4-isocyanatophenyl)methane
MEK	Methyl ethyl ketone
MPa	Megapascal
MPDI	1,3-Phenylene diisocyanate
PBS	Phosphate Buffered Saline

PCL	Polycaprolactone
PEO	Poly(ethylene oxide)
PPDI	1,4-Phenylene diisocyanate
PFG	Polyperfluoroether glycol
PIP	Piperazine
PPO	Poly(propylene oxide)
PTMO	Poly(tetramethylene oxide)
PU	Poly(urea)
PUU	Poly(urethaneurea)
QNM	Quantitative Nanomechanical Property Mapping
rpm	Revolutions per minute
SAXS	Small Angle X-ray Scattering
SS	Soft Segment
STPUUs	Segmented thermoplastic polyurethaneureas
TDI	Toluene diisocyanate
T_g	Glass transition temperature
THF	Tetrahydrofuran
T_m	Melting temperature
TPA	Terephthalic acid
TPEs	Thermoplastic elastomers
TPUs	Thermoplastic poly(urethaneurea)s
TSA	Tryptic Soy Agar
TSB	Tryptic Soy Broth
XPS	X-ray photoelectron spectrometer

CHAPTER 1

INTRODUCTION

1.1 Classification of Polymers

Polymer (from the Greek polys meaning "many" and meros meaning "part") was first used as a scientific term by the Swedish scientist, J.J. Berzelius in 1827. [5] Polymers, which are also termed as macromolecules, are long molecular chains composed of the repetition of many small molecules called *constitutional repeating units* or sometimes *monomers*, that are connected to each other by covalent bonds.

Polymers can be classified in many different ways. For example depending on their origins polymers can be classified as natural and synthetic. Based on their macromolecular architecture, chain structure or topology, polymers can be classified as linear, branched or cross-linked as shown in Figure 1.1. Linear polymers have two chain ends, while branched polymers have many chain ends depending on the extent of branching. In crosslinked polymers all chains are linked together by covalent bonds leading to a three dimensional network structure, which may also have a large number of end groups.

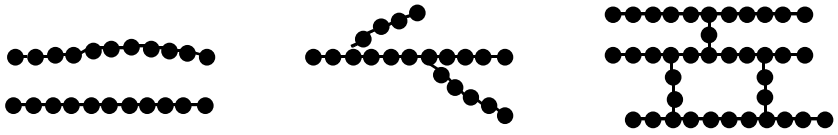

a) b) c)

Figure 1.1. Classification of polymers based on their macromolecular architecture, chain structure or topology. a) Linear polymer chains. b) Branched polymer chain. c) Cross-linked polymer chains. [6]

Depending on their mechanical properties polymers can be grouped as fibers, plastics and elastomers. An analysis of the behavior of fibers, plastics and elastomers can be seen in the stress–strain plots in Figure 1.2. The Young's modulus of a polymer is the initial slope of such a plot; the tensile strength and ultimate elongation are the highest stress and elongation

values, respectively. Elastomers are the group of polymers that can easily undergo very large, reversible elongations (500–1000%) at relatively low stresses. [7]

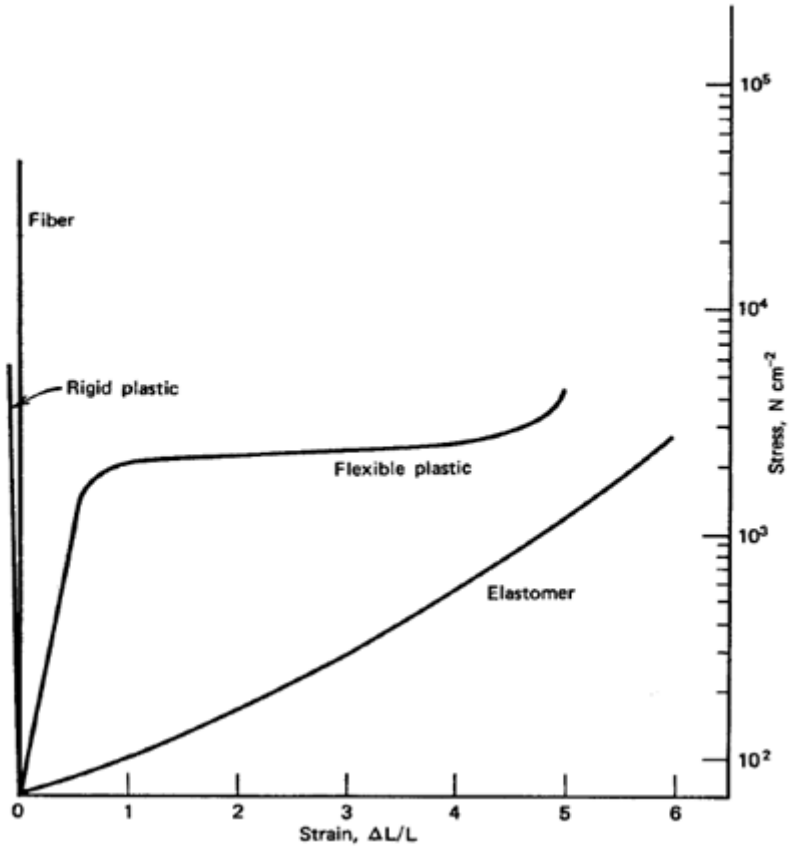

Figure 1.2. Stress–strain plots for a typical elastomer, flexible plastic, rigid plastic, and fiber. [7]

Depending on their chemical structures and compositions polymers can be classified as homopolymers, copolymers and terpolymers. Homopolymers consist of a single repeating unit or monomer, while copolymers and terpolymers are made of two and three different monomers respectively [7]. Depending on the arrangement of monomers in the polymer backbone, copolymers can be further classified as random, alternating and block copolymers. As their names imply, random copolymers consist of two randomly alternating monomers, alternating copolymers consist of two regularly alternating monomers, whereas block copolymers consist of two or more repeating homopolymer subunits linked together by covalent bonds as schematically shown in Figure 1.3.

a) ~~AAAAAAAAAAAAAAAAAAAA~~

Homopolymer

b) ~~ABABABABABABABABABAB~~

Alternating copolymer

c) ~~ABBBABBAABAAABABBBAAAB~~

Random copolymer

d) 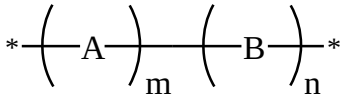

Block copolymer

Figure 1.3. The classification polymers depending on the arrangement of monomers. a) Homopolymers b) Alternating copolymers c) Random copolymers d) Block copolymers.

Block copolymers can further be divided into three sub groups depending on the number of blocks per macromolecule. As shown in Figure 1.4., these are diblock, triblock and multiblock copolymers [7].

AAAAAAAAAAAABBBBBBBBBB	A_nB_m	Diblock
AAAAAAAABBBBBBBBBBAAAAAAAA	$A_nB_mA_n$	Triblock
$(AAAAAABBBBBBB)_n$	$(A_nB_m)_p$	Multiblock

Figure 1.4. Schematic representation of di-, tri and multiblock copolymers.

Multiblock copolymers which are of interest of this study are also called segmented copolymers. Copolymer synthesis enables to controllably alter the properties of a desired homopolymer by introducing an appropriately chosen second polymer. By doing this, the

desired properties of homopolymers are combined in a single copolymer, therefore intense research activity continues in this area of polymer science with incredible numbers of repeating unit combinations being studied. [7-13]

When the chemical structures or molecular architectures are considered, commercially important thermoplastic elastomers are divided into two groups: (i) ABA type triblock copolymers, and (ii) $(A\text{-}B)_n$ type segmented (multiblock) copolymers. ABA type triblock copolymers consist of hard end blocks (A) and soft middle blocks (B), while segmented block copolymers consist of alternating hard and soft blocks as schematically shown in Figure 1.5. [14]. In this study our focus is on *segmented thermoplastic poly(urethaneurea)s* (STPUU), which sometimes are in general termed as thermoplastic polyurethanes (TPU). Block and segmented copolymers consisting of soft segments (SS) and hard segments (HS) are generally termed as thermoplastic elastomers (TPE).

Figure 1.5. Schematic representation of alternating soft and hard segments in segmented block copolymers.

As their name implies, SS provide softness and flexibility to the polymer as they are non-crystalline at ambient temperature and their T_g's are well below the ambient temperature. Similarly HS serves to increase the stiffness, toughness and affect other mechanical properties of the copolymer. They have a T_g or a crystalline melting temperature (T_m) much higher than ambient temperature. [8]

TPUU elastomers are a class of linear segmented elastic copolymers characterized by the presence of urethane and urea groups in their backbones. [15] Otto Bayer was the first scientist to suggest the synthesis of TPUUs by step-growth polyaddition reactions in 1937. [16] Later on Schollenberger described the preparation of elastomeric PUU fibers in 1955 [17], which was followed by the report published by Cooper and Tobolsky showing the microphase separated morphology of TPUs. [18] Since then TPUUs have gained considerable attention due to their interesting structure-property relationships. [19]

The bonds between the hard and soft segments are either in the form of urethane or urea, both of which are capable of hydrogen bonding. As shown in Figure 1.6, when the isocyanate groups react with hydroxyl and amine groups they form urethane and urea linkages respectively. Segmented TPUUs are generally synthesized by a two step polymerization technique, which is termed as the *prepolymer method,* which is discussed in Section 1.3.

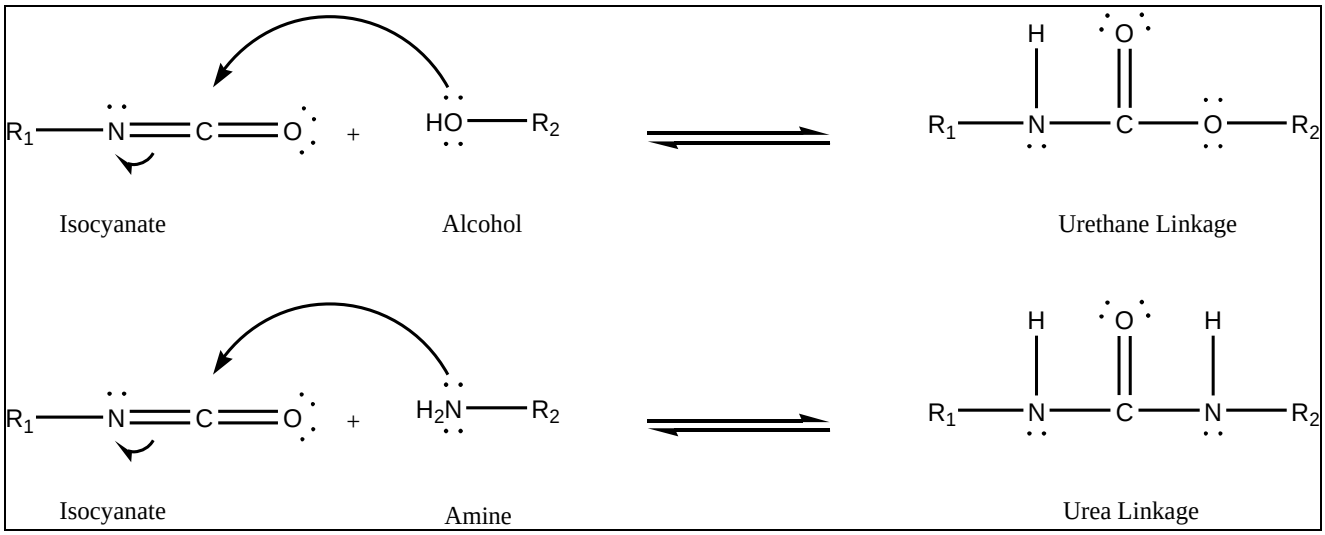

Figure 1.6. Formation of urethane and urea linkages through the reactions of isocyanates with alcohols and amines.

The polarity or solubility parameter differences between the HS and SS and the strong hydrogen bonding between the HS (urethanes and/or ureas) prevents the segments to mix with each other in molecular level. This results in a microphase separated morphology in TPUs. (Figure 1.7.) Although the blocks arrange themselves so they are microphase separated, they are still covalently linked. This results in interesting properties of these materials, which are strongly dependent on their chemical compositions and the resulting microphase morphologies. Depending on their hard/soft segment ratios TPUs may display properties ranging from elastomers to rigid plastics.

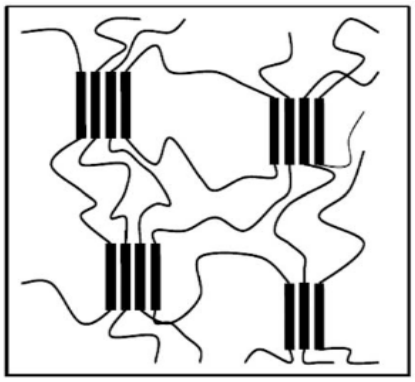

Figure 1.7. Schematic representation of microphase separation of HS and SS in TPU. The darker and thicker blocks are the HS, while the loose matrix is the SS. The HS strongly interact due to hydrogen bonding. [20]

1.2. Thermoplastic Elastomers

The fundamental requirement for an elastomer is the presence of highly mobile chain segments with anchoring sites at which chains are prevented from physically slipping past one another. When an elastomer is fully stretched, in the sense that further extension would rupture chemical bonds in the structure, its molecular chains will have been substantially aligned in the direction of the stretch. To ensure complete recovery from such large deformations, some inter linking of chains is essential to give a permanent three dimensional network structure but of a very loose nature [21]. What is required are some points of strong linkage between each chain and its neighbors, sufficient to stop slippage but not enough to interfere with the mobility of most segments of the chain. Most elastomers obtain the needed strength via covalent cross-linking and the incorporation of reinforcing inorganic fillers (e.g., carbon black, silica). [7] Vulcanization is one of the most popular techniques for this purpose. It is used to construct covalent bonds between polymer chains, therefore producing an elastomer which cannot be remolded into a different physical form. Therefore, conventional rubbers have to be cut to shape which involves a considerable amount of material waste. This disadvantage is overcome when thermoplastic elastomers are used.

Thermoplastic elastomers have physical rather than chemical linkages in between chains, therefore they have similar mechanical properties compared with vulcanized elastomers but at

the same time they can be heated and remolded several times. The strongest of these physical links are the intermolecular hydrogen bonds in between the HS of block copolymers.

1.3. STPUU synthesis

STPUUs are synthesized by a two step polymerization technique known as the *prepolymer method* as shown in Figure 1.8. In the first step of the synthesis an excess amount of diisocyanate is reacted with hydroxy terminated (or amine terminated) SS oligomers to form isocyanate terminated prepolymers. In the second step, isocyanate terminated prepolymers are reacted with stoichiometric amounts of diamine chain extenders (or diol chain extenders) to form the urea HS and high molecular weight TPUUs.

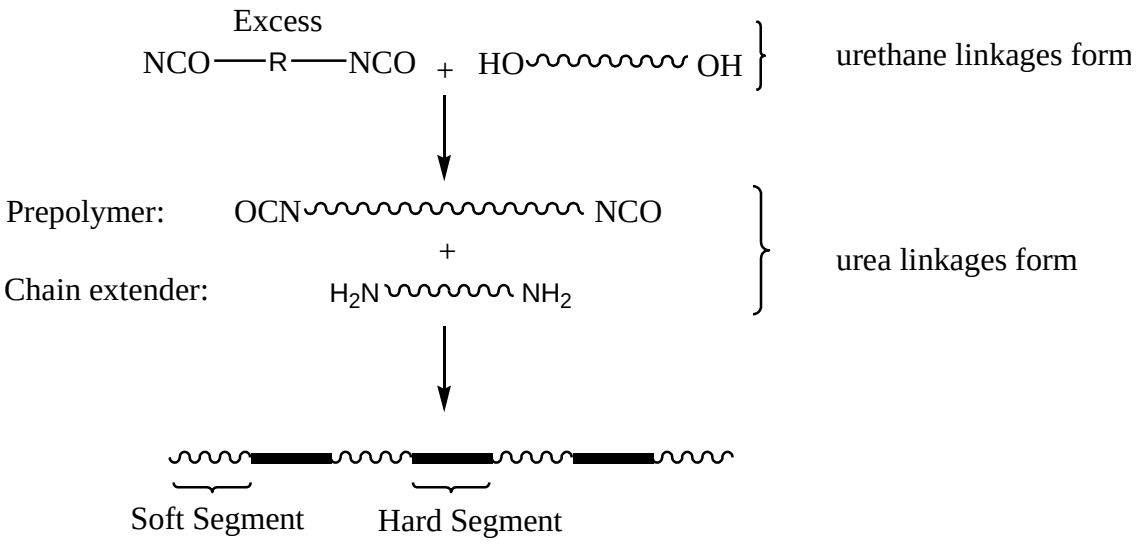

Figure 1.8. Representation of the two-step prepolymer method for the synthesis of segmented TPUU with alternating SS and HS along the copolymer backbone. [14]

In this study bis(4-isocyanatocyclohexyl)methane (HMDI) and 2-methyl-1,5-diaminopentane (MDAP) were used as the diisocyanate and the chain extender respectively, together with a variety of SS oligomers with different chemical structures, molecular weights and polarities. There was only one set of exception where hydroxyhexyl terminated polydimethylsiloxane (PDMS) was chain extended with 1,4 butanediol (BD) to obtain copolymers consisting of

only urethane linkages. The SS oligomers employed included poly(ethylene oxide)glygol (PEO), poly(propylene oxide)glycol (PPO), poly(tetramethylene oxide)glycol (PTMO), aminopropyl and hydroxyhexyl terminated polydimethylsiloxane oligomers (PDMS) and a polyperfluoroether glycol (PFG). Chemical structures of all starting materials are provided in Chapter 2.

1.4. Structure-Morphology-Property Relations in Segmented PUUs

A vast amount of starting materials is commercially available for TPUU synthesis. These include different diisocyanates, soft segment oligomers and chain extenders. As a result, in order to obtain the desired properties in TPUUs the design of the copolymer backbone -which includes the chemical composition, nature and the distribution of the SS and HS- plays a very critical role since it controls the microphase morphology of the copolymer. Control of the morphology of TPUUs are of particular interest because the nature and characteristics of the microphase separation determines the nano-structure of these segmented copolymers, which in turn controls the overall bulk and surface chemical and physical properties. Structure-morphology-property relations in STPUUs are schematically shown in Figure 1.9. There is a large number of parameters that influence the microphase morphology of TPUUs, which are discussed in detail below.

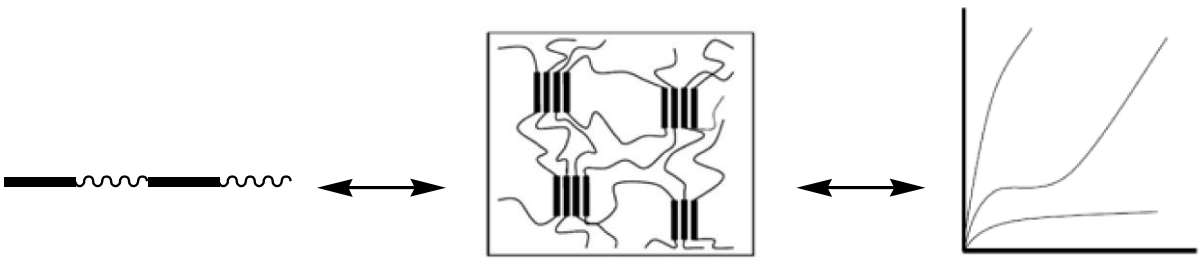

Figure 1.9. Schematic representation of the structure-morphology-property relations in segmented TPUUs.

1.5. Factors Affecting the Microphase Separation in Segmented PUUs

Very simply considered, the microphase separation primarily stems from; (i) the incompatibility of the SS and HS, (ii) the capacity of the HS to hydrogen bond, and/or (iii) crystallinity of the SS and/or HS. When the polarities of the HS and SS are close to each other, or if there is significant intermolecular interaction between them, phase mixing is more likely to occur. Whereas large polarity differences between SS and HS will most likely result in microphase separation. [22] As well known, the solubility parameters are a good indication for the polarity of a molecule. As the solubility parameter for a molecule increases, so does its polarity. Table 1.1. provides the solubility parameters of the SS and HS oligomers used in this study. Solubility parameter values given for the soft segments were obtained experimentally, while those for urethane and urea groups are calculated by using the group contribution method. [23, 24] As can be seen from this table, solubility parameters of the soft and hard segments are significantly different indicating the possibility of microphase separation in TPUUs.

Table 1.1. Solubility parameters of selected soft and hard segments. [23-28]

		Solubility parameter (δ) $(J/cm^3)^{1/2}$
Soft Segments	poly(ethylene oxide) (PEO)	20.2
	poly(propylene oxide) (PPO)	18.9
	poly(tetramethylene oxide) (PTMO)	17.6
	polydimethylsiloxane (PDMS)	15.6
	Poly(perfluoro ether) (PFE)	< 15
Hard Segments	urethane groups	37.2
	urea groups	45.6

In addition to the differences in the solubility parameters there are a large number of physical and chemical factors that have significant influence on the degree microphase separation in TPUUs. The most dominant ones are listed below: [14]

1- Chemical structure of the SS,
2- Number average molecular weight of the SS,
3- Hard/soft segment ratio in the copolymer,

4- Extent of competitive intermolecular interactions or hydrogen bonding between HS-HS and HS-SS,
5- Chemical structure and symmetry of the diisocyanate and HS,
6- Crystallizability of the HS and SS,
7- Processing conditions and thermal history of the copolymers.

1.5.1. Chemical Structure of the Soft Segments

The polyethers used in this study were poly(ethylene oxide), poly(propylene oxide) and poly(tetramethylene oxide). Due to the presence of fairly polar ether groups, there will be a competition for the hydrogen bonding between urethane-urethane or urea-urea in the HS and urethane-ether or urea-ether in the HS and SS in these copolymers. [8, 22, 23] This competition leads to some degree of phase mixing and strongly influences the overall thermal and mechanical properties of the resultant copolymer. [22] For a series of TPUU copolymers with identical HS compositions, those based on PEO are expected to contribute to phase mixing the most due to PEO's higher solubility parameter (20 $(J/cm^3)^{1/2}$) and higher concentration of ether groups in its backbone when compared with PTMO, which also has a somewhat lower solubility parameter of (17.6 $(J/cm^3)^{1/2}$). On the other hand depending on its average molecular weight PEO can crystallize and may lead to enhancement in the mechanical properties. PEO crystallites are thought to act as additional load bearing units, which are capable of absorbing strain energy. [9] Korley et. al., observed that introducing crystalline PEO units enhanced toughness and extensibility of TPUs compared with their amorphous analogs with the same amount of HS. [9] PEO based PUUs are also expected to be hydrophilic due to their polar nature. PTMO has also been reported to go under strain-induced crystallization under high strain rates. This behavior of PTMO SS, gives PTMO based copolymers very high TS values. [29]

The high polarity difference between the PDMS and urethane or urea HS result in an almost complete microphase separation in these systems. In copolymers composed of PDMS as SS; the lack of hydrogen bonding between the PDMS and urea segments leads to excellent microphase separation and therefore good mechanical properties. When amine terminated PDMS oligomers are used, formation of bidentate hydrogen bonds between the urea HS lead to enhancement in the thermal and mechanical properties. Presence of excellent microphase separation in PDMS based TPUUs was shown by Yilgor and co-workers both experimentally

[30] and also by dynamic molecular simulations [31] and quantum mechanical calculations [22].

Some interesting properties of TPUU copolymers synthesized using PDMS oligomers are their very low glass transition temperatures (-120 ˚C), high thermal, UV and oxidative stability, low surface energy, hydrophobicity, low coefficient of friction, high gas permeability, good electrical properties, physiological inertness, biocompatibility and very low surface tension values comparable to highly fluorinated polymers. [11, 28]

Fluorine based copolymers are also expected to show excellent microphase separation due to the extremely low solubility parameter of the polyperfluoroether glycol, (PFE, Fluorolink ® E10) SS. Since fluorine atoms linked to the carbon backbone repel each other in a symmetrical order, the dipole moments of fluorocarbon polymers are fairly low and highly non-polar. [32]

Another important factor that affects the mechanical performance of polyfluoroether containing copolymers is the existence of hydrogen atoms in their backbone. Generally fluoropolymers with hydrogen in their structures (i.e. Fluorolink® E10-H) have 1.5 times the strength and stiffness compared with fully fluorinated polymers and they are about twice as stiff. This is due to the strong intermolecular attractive forces between the CF_2 groups on one chain and the CH_2 groups on an adjacent chain. Also the alternating hydrogenated and perfluorinated units can interpenetrate during crystallization with the larger CF_2 groups on one chain “interlocking” with the smaller CH_2 groups on another chain. On the other hand, fully fluorinated chains lack this kind of “interlocking” therefore slip past each other. [32]

Fluorine has the highest electronegativity among all elements and the second smallest atomic radius after hydrogen. In a carbon-fluorine bond, a carbon atom is being strongly attracted by the most electronegative fluorine therefore generating a very strong and short covalent bond. The fluorine atom covers the carbon atoms without spacing therefore fluoropolymers are expected to have stiff spatial structures. [33]

The bond dissociation energy of the (C-F) bond which is known to be one of the highest can vary between 481-540 kJ/mol and the (C-C) bond energy rises from 348 kJ/mol in average to 360 kJ/mol in fluorocarbons. [32, 34, 35] This gives these polymers high UV, thermal and chemical stability. They are also characterized by their low frictional behavior due to their low surface energy and low molecular cohesion. [32] Fluorinated TPUs are also permeable to

oxygen and biocompatible due to their very low surfaces energies (23 mJ/m^2 for Fluorolink® E10-H), which imparts anti-adhesive character to a polymer. [35]

The comparison of the surface energies of polymers with surfaces composed of ordered single groups are: polyethylene (33.7 mJ/m^2), polydimethylsiloxane (21.2 mJ/m^2) and Fluorolink® E10-H (23 mJ/m^2). [35]

1.5.2. Effect of Soft Segment Molecular Weight

The average molecular weights of the SS incorporated into STPUU strongly influences their microphase morphology and overall properties. Average molecular weights of conventionally used SS are in 1,000-3,000 g/mol range. [8] Therefore soft segments with average molecular weights between 900-2,500 g/mol were chosen for this study.

It is intuitive that as the length of the SS increases, the distance between the hard domains should also increase and better microphase separation is achieved. This has been reported in many studies conducted with PUUs, some which will be discussed shortly. In copolymers with a fixed HS content, longer SS will reduce the effect of chain end junctions at the soft/hard segment interface and improve the mobility of the SS, leading to improved microphase separation.[8, 36]

In a study conducted by Wilkes, a series of poly(propylene glycol) (PPO) based PUUs were synthesized. The molecular weight of the PPOs used were 2000, 4000 and 8000 g/mol. Morphological features were studied with SAXS, AFM and thermomechanical analysis. The quantitative results of SAXS experiments showed that interdomain spacings increased with increasing molecular weight of PPO, as expected. For copolymers with fixed 6.3% by weight HS content, the interdomain spacings were found to be 120, 140 and 160 Å for PPOs that have an average molecular weight of 2000, 4000 and 8000 g/mol respectively. Also as another feature of the scattering studies was the increase in the intensity of the scattering curves as the molecular weight of the soft segmented increased, which pointed to a better microphase separation between hard and soft domains. It was further confirmed with AFM studies that better microphase separation was achieved with higher molecular weights of PPO. Thermal analysis showed increased soft segment molecular weights provided increased chain mobility and lower soft segment T_g's. [36]

Cooper and co-workers studied the effect of SS lengths on the rheological properties of TPU melts based on polycaprolactone (PCL) soft segments. As expected, the Newtonian viscosity and the relaxation time were very much dependent on block length. DSC, as well as SAXS, showed that samples based on PCL with $<M_n>$= 830 and 1,250 g/mol were single-phase materials. On the other hand, samples based on PCL with $<M_n>$= 2,000 and 3,000 g/mol were found to be increasingly microphase separated. [37]

Gaymans group studied the thermal and mechanical behavior of PPO based TPUs with $<M_n>$=1,000, 2,300 and 4,000 g/mol. They found that increasing the SS lengths decreased T_g, moduli and tensile strength. However, the decrease in the mechanical properties was mainly due to lower HS content in the copolymers. [38] In another study conducted by Hsieh et.al., copolymers with varying HS contents and SS lengths were prepared. Average molecular weights of SS were varied from 1,000 to 2,000 g/mol. Increased microphase mixing was observed due to an increase in the intermolecular interactions via hydrogen bonding for polymers with 1,000 g/mol SS molecular weights. [39] Yilgor and co-workers studied PDMS based TPUs and PUs by varying the SS block length. They found that SS blocks with 900 g/mol showed slight microphase mixing, whereas SS blocks with 2,500 and 7,000 g/mol were clearly microphase separated as confirmed with SAXS and DMA. [30]

1.5.3. Effect of the Hard Segment Content and Symmetry

It is expected that in PUUs an increase in the HS content or molecular weight will lead to an improvement in microphase separation. In addition, since HS provides stiffness and strength while the SS incorporate softness and flexibility to PUUs, the modulus and tensile strength values are expected to increase as the HS content increases.[39] It was also demonstrated that the tensile strengths of PDMS based PU copolymers increase linearly with the HS content of the copolymer. [22] SAXS studies on PUUs [40] clearly showed that an increase in the HS content improved the microphase separation up to about 60% wt HS content. Interestingly an increase in the microphase mixing was observed in PUUs containing higher 60% by weight HS, probably due to kinetic constraints in HS packing. [40, 41] On the other hand more recent studies showed that the degree of microphase separation was almost constant for PUUs with HS contents between 50-90% wt. [42]

Barikani et. al., investigated the effect of the chemical structures of various isocyanates on the softening temperatures of a series of 1,4-butanediol (BD) chain extended TPUs. The HS content of these TPUs were 20% by weight. Diisocyanates used for this purpose were; PPDI (1,4-phenylene diisocyanate), MDI (p-Diphenylmethane diisocyanate), CHDI (1,4-cyclohexyl diisocyanate), HMDI (Bis(4-isocayanatocyclohexyl)methane) and TDI (2,6- and 2,4- Toluene diisocyanate) while PCL (polycaprolactone) was used as the SS. [43] As can be seen from Figure 1.10, there is a dramatic difference in the rubbery plateau modulus among the materials produced using symmetrical diisocyanates such as (CHDI and PPDI) when compared to the less symmetric or asymmetric diisocyanates (MDI, HMDI and TDI). This work demonstrated that the isocyanate structure and symmetry played an important role in the properties of TPUs, however the significant difference in the glassy state moduli depending on the diisocyanate symmetry was not discussed by the original researchers. [8]

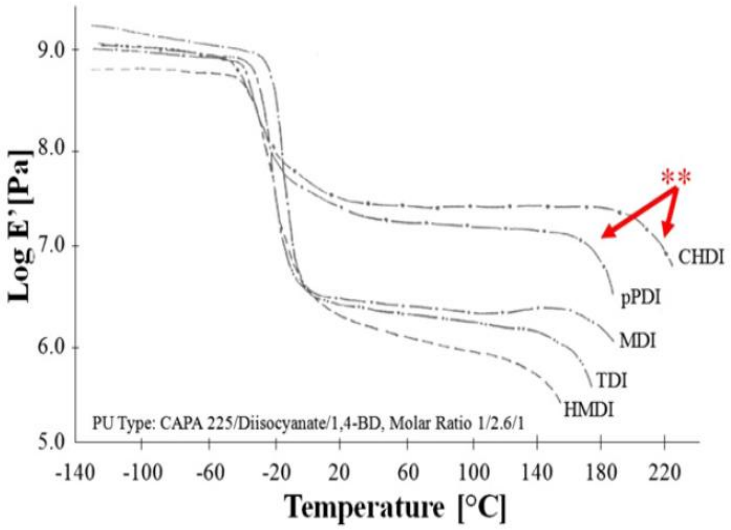

Figure 1.10. DMA behavior of TPU based on PCL, various diisocyanates chain extended with BD containing 20%wt HS. [43]

Yilgor and Wilkes extended these studies by preparing TPUs through the stoichiometric reactions between PTMO-1K and various diisocyanates, including CHDI, PPDI, MPDI (1,3-Phenylene diisocyanate), MDI and HMDI. [13] Characterization studies clearly showed that while symmetric PPDI and CHDI based TPUs and PUs showed self organization and excellent microphase separation, no phase separation was observed for asymmetric MDI and

HMDI based TPUs. [13] A complementary review on *non-chain extended* TPUs and PUs based on PTMO-1K SS and CHDI, HDI, PPDI, HMDI and MPDI was also published [14]. The nature and extent of microphase separation was investigated by FTIR, AFM, SAXS and DMA. TPUs based on symmetric isocyanates showed good mechanical integrity and phase separation at room temperature while TPUs based on asymmetric isocyanates did not form films with mechanical integrity at room temperature. AFM pictures showing microphase separation of TPU based on symmetric isocyanates are presented in Figure 1.11.

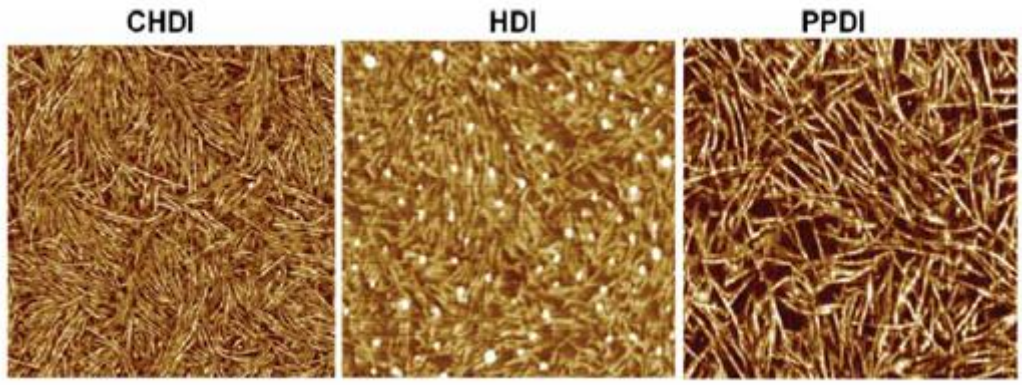

Figure 1.11. AFM images of *non chain extended* TPUs based on PTMO-1K and corresponding highly symmetrical diisocyanates. Full scale at each AFM picture is 2 μm.[14]

On the other hand homologous segmented PUs based on PTMO-1K and asymmetric diisocyanates (HMDI and MPDI) did form films with good mechanical integrity at room temperature. However symmetrical diisocyanates (PPDI, CHDI and HDI) showed more distinguished microphase separated morphologies and better tensile properties. AFM images of selected PUs are provided on Figure 1.12. As will be discussed in the next section, urea forms stronger bidentate hydrogen bonding when compared with monodentate urethane bonds, which results in improved microphase separation and therefore stronger mechanical properties.

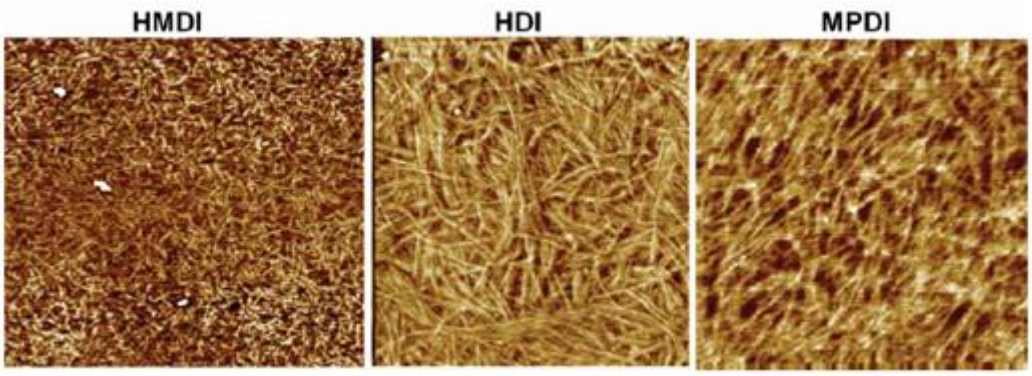

Figure 1.12.AFM phase images of *non chain extended* PUs based on PTMO-1K and corresponding diisocyanates. Full scale at each AFM picture is 2 μm. [14]

1.5.4. Hydrogen Bonding

One of the most important factors that contribute to the microphase separation in TPUUs is the nature and strength of the hydrogen bonding between the urethane or urea HS. When hydrogen bonding strictly takes place between HS, excellent microphase separation is observed. It was shown that improved microphase separation results in increased tensile strengths and elongations compared to polymers with similar compositions which are not microphase separated. [22]

In urethane and urea groups hydrogen bonding primarily takes between the hydrogen atom on an N─H group and the oxygen atom on the carbonyl C=O group. As shown in Figure 1.13, due to its bidentate nature, the hydrogen bonding between urea groups are much stronger compared to those between urethanes. This is because urea groups have two N─H groups per carbonyl, whereas the urethane groups have only one, forming only monodentate hydrogen bonds.

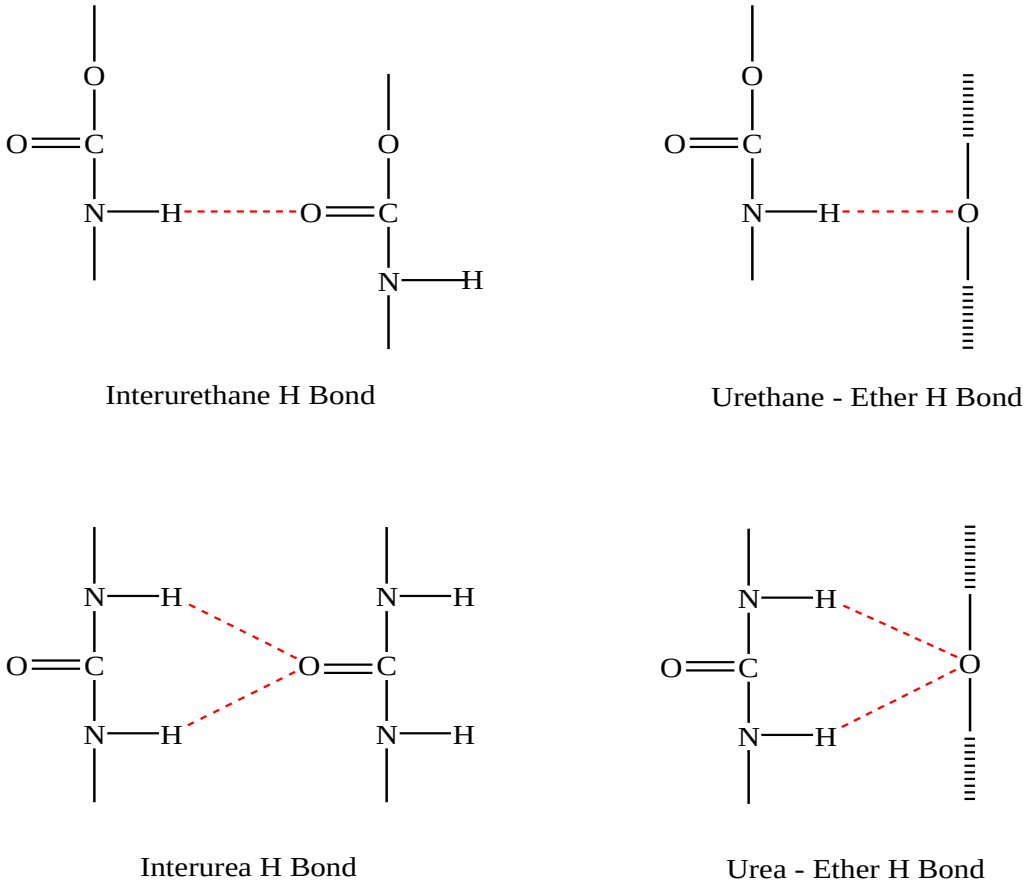

Figure 1.13. Monodentate and bidentate hydrogen bonding between urethane, urea and ether groups.

When hydrogen bonding between HS are disturbed due to the ability of the SS (such as polyethers or polyesters) to hydrogen bond through ether or ester linkages as shown in Figure 1.13, microphase separation is also disturbed. This strongly influences the mechanical properties and overall performance of TPUUs.

Quantum mechanical calculations have also shown that the bidentate hydrogen bonding between urea groups (65.1 kJ/mol) are much stronger when compared with that between the urethane groups (46.5 kJ/mol). Therefore segmented copolymers containing urea linkages are expected to have better microphase separation and improved mechanical properties compared to polymers containing urethane linkages [14, 23], which has been demonstrated by FTIR, AFM, SAXS and DMA studies involving a wide range of STPUs based on different diisocyanates as discussed previously. [14, 25, 44]

Gaymans demonstrated the effect of hydrogen bonding on morphology and mechanical properties of segmented polyamides. Copolymers were prepared using PTMO-1K and PTMO-2K as the SS and hydrogen bonding and non-hydrogen bonding crystallizable polyamide HS with uniform lengths. The HS were obtained by the chemical combination of terephthalic acid (TPA) and hexamethylene diamine (HMDA) or piperazine (PIP) respectively. As can be seen in Table 1.2. the tensile strengths of the copolymers with strongly hydrogen bonding HMDA based hard segments were substantially higher when compared with copolymers containing PIP based HS. These results clearly demonstrate the dramatic effect of intermolecular hydrogen bonding between the HS on the mechanical properties of segmented elastomeric polyamides. [45]

Table 1.2.

Effect of hydrogen bonding on the tensile properties of segmented polyamides with crystalline HS.

Polymer Description	Hard segment content (wt%)	Elastic modulus (MPa)	Ultimate Tensile Strength (MPa)	Elongation at break (%)
PTMO-1k/PIP	32.5	140	28	640
PTMO-1k/HMDA	35.0	330	38	470
PTMO-2k/PIP	19.8	33	22	1050
PTMO-2k/HMDA	21.6	110	33	700

In another study when the hydrogens in the amide groups of a polyamide-6,10 are selectively replaced with tertiary butyl groups, a dramatic reduction in the modulus of the materials were observed. When the logarithm of the modulus was plotted against the level of substitution in these polyamides a straight line was observed as shown in Figure 1.14. When the line is extrapolated to 100% substitution, negative log(modulus) values are obtained clearly indicating that in the absence of hydrogen bonding polyamide-6,10 would be a very soft and weak material. These results clearly show that the stiffness and strength in these materials are a direct result of hydrogen bonding of the system. [46-48]

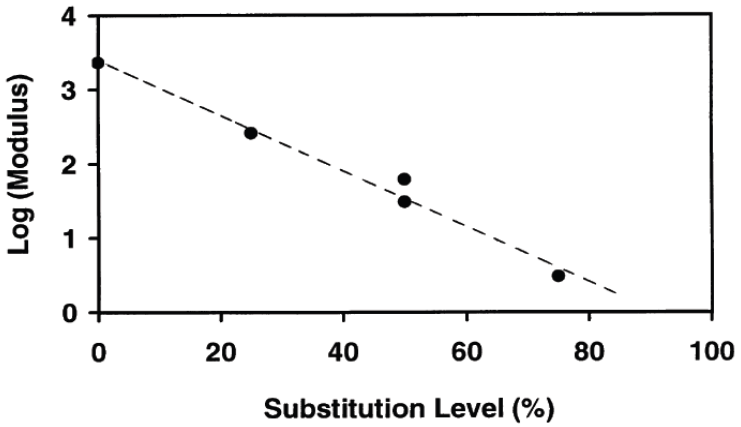

Figure 1.14. Influence of level of N-substitution on the modulus of polyamide-6,10. [22]

1.5. Biomedical Applications of Thermoplastic PUUs

PUUs were first proposed to be used as biomaterials in 1967 by Boretos and Pierce as heart assist systems. [49] From that date on, diamine chain-extended PUUs have been widely used in medical applications. Some of their most common applications include biomedical devices, implants, artificial blood vessels and wound dressing applications due to their superior mechanical properties, blood compatibility, oxygen permeability and their ability to be engineered according to application. [1, 15] One other interesting application of segmented TPUU copolymers in the last decade is their usage as advanced drug delivery systems. The solubility difference between the HS and SS allows for drugs to be incorporated in the hydrophobic sections while the hydrophilic sections are subjected to aqueous solutions *in vivo*. [50] However, when introduced *in vivo* conditions, some of the conventional TPUs can fail. Also the unpredicted biodegradation has ended up in some cases where the patient was subjected to toxic materials. [51] These are serious problems considering TPUUs are extensively being used as cardiac pacemaker leads, breast implants, vascular devices, artificial heart implants, and heart valves. [52] Therefore it is vital for TPUUs to be characterized in depth before they are proposed for any kind of biomedical application. Various studies on characterizing TPUUs for biomedical applications have been conducted.

Kanyanta et.al., characterized the change of mechanical properties of ether based TPUs elastomers by varying temperature, humidity and strain rate. [15] Their purpose with varying these parameters was to mimic *in vivo* conditions. Another study conducted by Bil et.al., varied the HS content of aliphatic poly(ester urethanes) from 22 to 70% by weight and

characterized their microphase separation, mechanical and surface properties for bone tissue engineering applications. [12] It has also been demonstrated that the biostability of the TPUUs is closely related to the HS content, microphase separation and ability of SS to crystallize upon stress. [51] Tang et.al., synthesized polycarbonate based TPUs by varying the HS to study the biodegradation of PU materials. [53] It was shown that the biodegradation of TPUs was closely dependent on the HS chemistry, microphase morphology and strength and extent of the hydrogen bonding within the HS. [51] These findings clearly suggested that the strength of hydrogen bonding was an important parameter to consider in the design of biostable TPUUs. [51]

Another approach to improve biocompatibility and reduce hydrolysis was surface modification of the TPUUs by the incorporation of small amounts of PDMS or polyfluoroether oligomers. [54] Fluorinated or PDMS based TPU are commonly used for contact lenses, dental materials and surgical adhesives. Fluorourethanes are also used to construct an intra-aortic balloon catheter and as hydrophobic microporous membranes used in breathable, sterile fabrics. [35]

1.6. Biofilm formation on polymer surfaces and studies on their inhibition

Recent publications have clearly stated the necessity for developing strategies for reducing bacterial adhesions on medical devices, especially on endotracheal tubes. [55, 56] One of the greatest risk factors for ventilator associated pneumonia (VAP) is born from prolonged endotracheal intubation and this type of pneumonia can be fatal especially for kids and elder patients. [57] Currently medical-grade poly(vinyl chloride) (PVC) is used as the material for endotracheal tubes. [58] PVC offers a perfect environment in which bacterium can stick on it and form mature biofilms within a couple of hours or days. These biofilms secrete a mucosa-like extracellular polymeric substance that prevents the penetration of the antibiotics within its structure. This makes them extremely resistant to medication and results in VAP in patients. 86% of VAP are reported to be associated with mechanical ventilation and 40% of these cases are reported to be fatal despite aggressive antibiotic therapy. [58, 59] Not only does this affect the health of the patient, but it also prolongs the time the patient has to be treated in the hospital, causing additional expenses.

Bacterial attachment to a solid surface is highly dependent on the surface properties of the material; such as its chemical composition and reactivity, surface energy and hydrophobicity, surface roughness, and porosity. [2] Therefore, several attempts have been being made to surface modify PVC.[58] The exact sticking mechanism of bacterium on solid surfaces are not clear and also it is known that different bacterium strain have different mechanism of sticking on solid surfaces [2]. There have been suggestions in the literature that hydropobicity reduced biofilm formation [3], however there have also been opposite opinions where the authors suggest that hydrophilicity reduced biofilm formation [2]. In this thesis we have tested several polymers with varying surface energies and chemical compositions to observe if the difference in surface energy, and consequently wettability, will result in reduced biofilm formation.

1.7. Purpose of the Study

Due to their interesting combination of bulk and surface properties segmented TPUUs find wide range of applications in many diverse fields, which include textile fibers, membranes, adhesives, automotive plastics and others. One of the emerging applications of TPUUs include their use as biomaterials. This is mainly due to the possibility of designing and synthesizing TPUUs with controlled bulk and surface properties that possess very good blood and tissue compatibility as will be discussed in detail further on. [60]

The main goals of this study were the investigation of the influence of;

(i) SS structure,
(ii) SS molecular weight, and
(iii) HS content

on the morphology and the bulk and surface properties of TPUUs. In addition, another aim was to investigate the effect of the polymers surface energies on the amount of biofilm formation. For this purpose, biofilms were grown on the surfaces of different polymers. These biofilms were then quantized and compared.

For characterization purposes TPUUs based on five different SS were synthesized and characterized. The chemical structures of the HS of these copolymers were kept identical with one exception, when the chain extender was changed from MDAP to BD in copolymers based on hydroxyhexyl terminated polydimethylsiloxane (PDMS).

Five different SS used for this study included PEO, PPO, PTMO, aminopropyl and hydroxyhexyl terminated PDMS and a polyfluoroether (Fluorolink E10-H®). Bis(4-isocyanatocyclohexyl)methane (HMDI) was used as the cycloaliphatic diisocyanate and 2-methyl-1,5-diaminopentane (MDAP) or 1,4 butanediol (BD) was used as the chain extender.

PEO, PPO and PTMO were chosen to understand the effect of polyether backbone and polarity on morphology and bulk and surface properties of TPUUs. To investigate the influence of the molecular weight, SS oligomers with two different molecular weights of 1,000 and 2,000 g/mol with some exceptions were used during the synthesis. HS contents of the copolymers were also kept constant at 20 and 30% by weight with some exceptions.

CHAPTER 2

EXPERIMENTAL

2.1. Materials

Bis(4-isocyanatocyclohexyl)methane (HMDI) with a purity better than 99.5% by weight was kindly provided by Bayer AG, Germany and was used as received. Poly(ethylene oxide)glycol (PEO) with $<M_n>$ = 1000 and 2000 g/mol (Merck); poly(propylene oxide)glycol (PPO) with $<M_n>$ = 1000 and 2030 g/mol (Acclaim by Bayer); poly(tetramethylene oxide)glycol (PTMO) with $<M_n>$ = 985 and 2040 g/mol (DuPont); aminopropyl terminated poly(dimethyl siloxane) (PDMS A-Si 2120) $<M_n>$ = 980 g/mol, (PDMS A-Si 2320) $<M_n>$ = 2500 g/mol (Goldschmidt AG); hydroxyhexyl terminated poly(dimethyl siloxane) (PDMS H-Si 2111) $<M_n>$ = 1000 g/mol, (PDMS H-Si 2311) $<M_n>$ = 2500 g/mol (Goldschmidt AG); polyperfluoroether glycol (PFE) $<M_n>$ = 1400 g/mol (Fluorolink® E10-H, Solvay Solexis) were used as received. 2-Methyl-1,5-diaminopentane (MDAP) (DuPont) and 1,4-butanediol (BD) (Merck) were used as chain extenders without any purification. Dibutyltindilaurate (DBTDL) was obtained from Air Products and was used as a catalyst as a 1% by weight solution in THF for all synthesis, except for PFE and hydroxyhexyl terminated PDMS based polymer synthesis when it was used neat. Reagent grade tetrahydrofuran (THF), dimethylformamide (DMF) and isopropanol (IPA) were purchased from Merck, methyl ethyl ketone (MEK) was purchased from LAB-SCAN Analytical Sciences and used as received. The chemical structures of the reagents used are provided in Table 2.1.

Table 2.1. Chemical structures of the reactants.

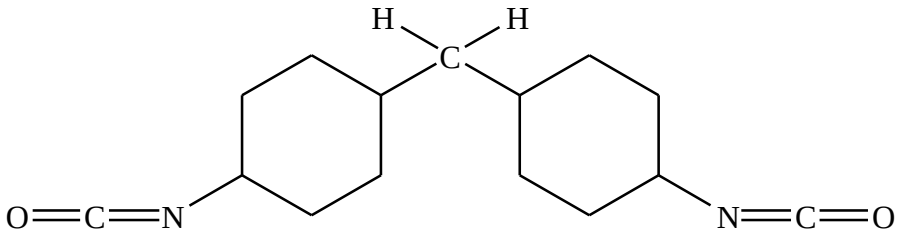

HMDI: Bis(4-isocyanatocyclohexyl)methane, M_n = 262.35 g/mole.

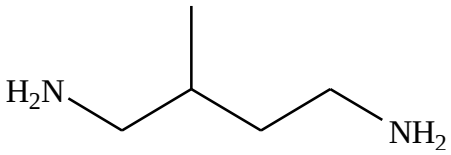

MDAP: 2-Methyl-1,5-diaminopentane, M_n = 116.2 g/mole.

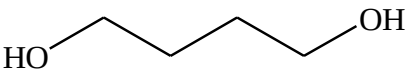

BD: 1,4-Butanediol, M_n = 90.12 g/mole.

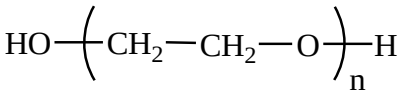

PEO: Poly(ethylene oxide) glycol

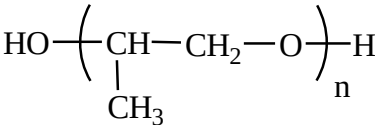

PPO: Poly(propylene oxide) glycol

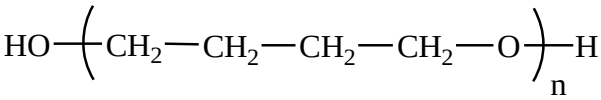

PTMO: Poly(tetramethylene oxide) glycol

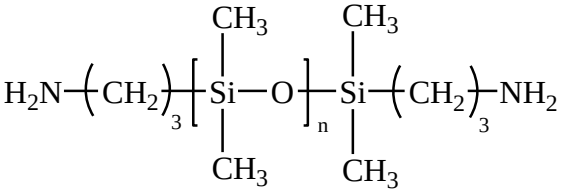

N-PDMS: α,ω-Aminopropyl terminated polydimethylsiloxane

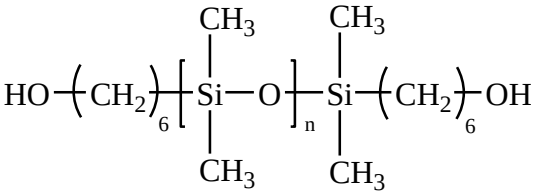

H-PDMS: α,ω-Hydroxyhexyl terminated polydimethylsiloxane

$HO(CH_2CH_2O)_nCH_2CF_2O(CF_2CF_2O)_p(CF_2O)_qCF_2CH_2(OCH_2CH_2)_nOH$

PFE: Polyperfluoroether glycol

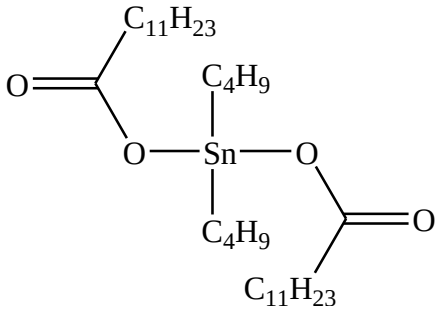

DBTDL: Dibutyltindilaurate

2.2. Polymer Design and Calculations Used for Determining the Reaction Stoichiometry

Depending on the soft segment molecular weight and the hard segment content of the TPU or PUU segmented copolymer to be synthesized, one of the critical design parameters is the determination of the reaction stoichiometry. An exemplary calculation is provided below for the preparation of 5.0 g of a segmented PUU based on PEO-1000, HMDI and MDAP, containing 30% by weight hard segment.

Total amount of the hard segment (HMDI+MDAP) in grams of a 5 gram copolymer with 30% by weight hard segment will be:

5 x 0.3 = 1.5 grams of (HMDI+MDAP)

Amount of PEO-1000 will be: 5.0 -1.5 = 3.5 grams

Number of moles of PEO to be used is: $3.5/1000 = 3.5x10^{-3}$ mole.

In order to obtain a high molecular weight polymer, number of moles of HMDI to be used should to be equal to the total number of moles of PEO-1000+MDAP.

If number of moles of MDAP is taken as (a) moles, then the number of moles of HMDI needed should be: $a + 3.5x10^{-3}$ moles. Since the total amount of HMDI+MDAP is 1.5 g, then:

$[(a + 3.5x10^{-3}) \times (262.35)] + [a \times 116.2] = 1.5$ grams.

From here number of moles of MDAP or (a) is found to be: $1.53x10^{-3}$ mole, and its weight in grams will be: $1.53x10^{-3}$ mole x 116.2 g/mole = 0.18 grams

Then the number of moles of HMDI is calculated to be: $1.53x10^{-3} + 3.5x10^{-3} = 5.03x10^{-3}$mole, or its weight in grams will be: $5.03x10^{-3}$ mole x 262.35 g/mole = 1.32 grams.

Then the reaction stoichiometry for the preparation of a PUU based on PEO-1000, HMDI, MDAP with a hard segment content of 30% by weight will be as follows:

[HMDI]/[PEO-1000]/[MDAP]= 5.03/3.5/1.53

2.3. Description of the General Reaction Procedure Used for the Preparation of SPUU Copolymers

General procedure for the copolymerization reactions were as follows: All synthesis reactions were conducted by using the conventional two step “prepolymer” method as has been described previously. [14] Reactions were carried out in a 100 or 250 mL, 3-neck round bottom Pyrex flask equipped with an overhead stirrer, thermometer and addition funnel. Reaction flask was heated by a heating mantle. In the first step in order to obtain an isocyanate terminated “prepolymer”, the hydroxyl or amine terminated soft segment oligomers were reacted with a stoichiometric excess of HMDI, which was determined by using the calculation explained above. Reaction of HMDI with hydroxy terminated oligomers was conducted in bulk, at 60-80 °C range, under the catalytic action of DBTDL. DBTDL is known to exhibit remarkable catalytic activity for the reaction between isocyanate and

compounds bearing a labile hydrogen atom. [61] Prepolymer formation reactions of HMDI and amine terminated oligomers were carried out in solution at room temperature without using a catalyst. In the second step, chain extension was accomplished by the dropwise addition of MDAP or BD dissolved in an appropriate solvent. All chain extensions, where MDAP was used, were conducted at room temperature, whereas chain extension reactions of BD was performed at 80 °C. If the polymer is *non-chain extended* the synthesis is conducted in one step. HMDI is weighed in the round bottom Pyrex flask and stoichiometric amount of the soft segment in solution is dropwise added on top of it while stirring is taking place and polymerization is finished by the end of this addition. This process can be at RT or elevated temperatures depending on the composition.

Progress and completion of the polymerization reactions were monitored by using Fourier Transformation Infrared (FTIR) spectroscopy. During the reactions, samples were withdrawn from the reaction mixture at different reaction times and their FTIR spectra were obtained. The prepolymer formation was monitored by the disappearance of the hydroxyl peak around 3500 cm^{-1} and formation of urethane N-H and C=O peaks around 3300 and 1700 cm^{-1} respectively. Chain extension reactions were stopped upon the disappearance of the strong isocyanate peak at 2270 cm^{-1}. In general approximately 70-80% of the chain extender solution was used due to side reactions consuming excess isocyanate during prepolymer formation, which is well documented in the literature. [61-63]

After polymer syntheses were completed, the polymer solutions were poured in Teflon molds and kept inside a hood at room temperature in order to allow the slow evaporation of the solvent. Following this, they were dried in a vacuum oven at 60 °C until constant weight was achieved. Film samples were kept in sealed polyethylene bags at room temperature.

2.3.1. Synthesis of PEO based PUUs

For the prepolymer synthesis calculated amounts of PEO and HMDI were weighed into the reaction flask. Mixing was initiated at around 120 rpm while the flask was being heated. Once the desired temperature of approximately 60 °C was established, two drops of catalyst solution (1% wt of DBTDL in THF) was added. As described earlier, the reaction was followed by FTIR spectroscopy. Depending on the viscosity of the prepolymer mixture obtained, THF was added to give a final concentration of about 60-70% by wt. The

prepolymer reaction was continued for approximately 90 minutes. Once the formation of prepolymer was accomplished, the heating mantle was removed and the prepolymer solution was cooled down to room temperature.

In the chain extension step, MDAP solution in DMF (at a concentration of 5% wt solids) was added dropwise into the isocyanate capped prepolymer solution at room temperature under strong agitation. As the viscosity of the solution increased, it was diluted by the addition of DMF. The reaction was continued until the disappearance of the strong isocyanate peak in FTIR spectrum. The chain extension step took approximately 60 minutes.

2.3.2. Synthesis of PPO based PUUs

Calculated amounts of PPO and HMDI were weighed into the Pyrex reaction flask. Mixing was initiated at around 120 rpm while the flask was being heated. Once the desired temperature of approximately 80 °C was established two drops of catalyst solution (1 % wt of DBTDL in THF) was added. The prepolymer formation reaction was conducted in bulk. The reaction was followed by FTIR spectroscopy. The prepolymer formation reaction was completed in approximately 50 minutes. Then the heating mantel was removed to allow cooling and THF was added to obtain a 50% by wt prepolymer solution. IPA was added as a co-solvent onto the cooled prepolymer solution to increase the polarity of the mixture before chain extension reaction.

In the second step MDAP solution in IPA (at a concentration of 5% wt solids) was added dropwise onto the isocyanate terminated prepolymer solution at room temperature under strong agitation. IPA was used for dilution if necessary. The reaction was followed by FTIR spectroscopy and the addition of MDAP was stopped upon the disappearance of the strong isocyanate peak located at 2270 cm^{-1}.

2.3.3. Synthesis of PTMO Based PUUs

The synthesis of PTMO based PUUs were performed in exactly the same way as the PPO based PUU synthesis described in 2.3.2.

2.3.4. Synthesis of PDMS Based PU and TPUs

2.3.4.1. Synthesis of PDMS Based PUs

Aminopropyl terminated PDMS was dissolved in IPA to obtain a 50% by weight solution and was placed into an addition funnel. This solution was added dropwise into the Pyrex reaction flask where calculated amount of HMDI was previously introduced. The addition was completed at room temperature in approximately 15 minutes without the need of a catalyst.

The chain extension step was performed in the same manner as was described for PPO based PUUs.

2.3.4.2. Synthesis of PDMS Based TPUs

Calculated amounts of hydroxyhexyl terminated PDMS and HMDI were weighed into a Pyrex reaction flask. Mixing was initiated at around 120 rpm while the flask was being heated. Once the desired temperature of approximately 80 °C was established one drop of neat DBTDL was added. The prepolymer was conducted in bulk at approximately 90 minutes.

In the second step BD solution in MEK (at a concentration of 5% wt solids) was added dropwise on the isocyanate terminated prepolymer at 70-75 °C under strong agitation. MEK was used for dilution if necessary. The reaction was followed by FTIR spectroscopy. The chain extension solution was added at 6 hours. The reaction was completed at approximately 26 hours.

2.3.5. Synthesis of PFE Based PUUs

PFE based PUUs were synthesized in exactly the same way as the PPO based PUUs, with the exception that the chain extension step took place at approximately 60 °C.

Table 2.2

Chemical compositions and hard segment molecular weights of segmented polyurethane, polyurea and polyurethaneurea copolymers synthesized in this study

(*) Calculated from reaction stoichiometry

Copolymer Designation	Soft segment		Chain Extender	Hard segment		Reaction Solvent
	Type	$<M_n>$ g/mol		Content (wt %)*	$<M_n>$ g/mol*	
PEO1-UU-30	PEO	1000	MDAP	29.4	1,053	THF/DMF
PEO2-UU-20	PEO	2000	MDAP	19.9	840	THF/DMF
PEO2-UU-30	PEO	2000	MDAP	27.9	819	THF/DMF
PPO1-UU-30	PPO	1000	MDAP	29.3	912	THF/IPA
PPO2-UU-20	PPO	2000	MDAP	19.6	982	THF/IPA
PPO2-UU-30	PPO	2000	MDAP	30.0	900	THF/IPA
PTMO1-UU-25	PTMO	1000	MDAP	24.9	1,930	THF/IPA
PTMO1-UU-30	PTMO	1000	MDAP	28.4	1,820	THF/IPA
PTMO2-UU-20	PTMO	2000	MDAP	19.2	1,179	THF/IPA
PTMO2-UU-30	PTMO	2000	MDAP	28.8	787	THF/IPA
H-PDMS1-Ur-30	H-PDMS	900	BD	30.4	912	MEK
H-PDMS2.5-Ur-20	H-PDMS	2500	BD	21.0	659	MEK
H-PDMS2.5-Ur-30	H-PDMS	2500	BD	30.9	1,114	MEK
A-PDMS1-U-22.5	A-PDMS	900	-	22.5	262	IPA
A-PDMS1-U-30	A-PDMS	900	MDAP	29.9	1,389	IPA
A-PDMS2.5-U-20	A-PDMS	2500	MDAP	21.3	811	IPA
A-PDMS2.5-U-30	A-PDMS	2500	MDAP	30.6	1,104	IPA
PFE1.4-Ur-16	PFE	1400	-	16.0	262	THF/IPA
PFE1.4-UU-20	PFE	1400	MDAP	20.2	1,341	THF/IPA

2.3.6. Nomenclature System for the Copolymers Synthesized

Types and the molecular weights of the soft segments, type of the chain extender and reaction solvents used, chemical compositions, hard segment molecular weights and contents of the copolymers prepared together with their nomenclature are provided on Table 2.2.

The nomenclature or coding of the samples were as follows: First three to five letters are used to identify the SS (e. g. PEO for poly(ethylene oxide) and HPDMS for hydroxyhexyl terminated PDMS), the numbers that followed these letters indicated the average molecular weights of the SS in kg/mol. UU, U and Ur indicated the type of the hard segment as urethane-urea, urea and urethane respectively. The final number showed the HS content of the copolymers in weight percent.

2.4. Characterization Methods

2.4.1. Spectroscopic Analysis

Samples for FTIR analysis were prepared by smearing polymer solutions on KBr discs and evaporating the solvent with a heat gun resulting in thin polymer films. Nicolet Impact 400 D spectrometer equipped with a DTGS-KBr detector was used for analysis. 32 scans were taken for each spectrum with a resolution of 4 cm^{-1}.

Polymer films prepared by solvent casting on Teflon molds as described in 2.1. were directly used for Attenuated Total Reflection Fourier Transform Infrared (ATR-FTIR) spectroscopic studies. The measurements were performed under ambient temperatures by using a Nicolet iS10 spectrometer. The spectrometer was equipped with a flat diamond plate and measurements were collected at an angle of 42°. 16 scans were obtained for each spectrum with a resolution of 4 cm^{-1}.

2.4.2. Stress-Strain Tests

Dog-bone shaped specimens were cut from solvent cast polymer films according to ASTM D-1708 standards. Tests were performed on an Instron Model 4411 Universal Tester at ambient temperatures with a cross-head speed of 25.0 mm/min. Original lengths (L_o) of the test specimens were 25.0 mm. A minimum of three samples for each polymer film were tested for Young's modulus, tensile strength and elongation at break.

2.4.3. Atomic Force Microscopy

Atomic force microscopy (AFM) studies were undertaken using Bruker Dimension Icon AFM. All copolymers scans were performed in tapping mode except the PFE based

copolymers scans which were performed using QNM mode. Both height and phase images were recorded. The tip of the probe used for the tapping mode has a spring constant of 40 N/m and a resonant frequency of 300 kHz. The tip of the probe for the QNM mode has a spring constant of 0.4 N/m and a resonant frequency of 70 kHz. Solvent cast polymer films were put in vacuum at RT for 12 hours prior to AFM studies. Height and phase images were simultaneously recorded of sample surfaces.

2.4.4. Small Angle X-ray Scattering

Polymer films that had been prepared by solvent casting were cut to fit the sample holder. Bruker D8 Advanced X-Ray Diffractometer was used for analysis. All measurements were conducted using a Cu-Kα X-ray source and parallel beam geometry resulting in a wavelength (λ) of 1.5406 Å. 0.1 mm divergence slit was used after goebel mirror. 0.1 mm slit was used by the detector. Scintillation detector was used for all measurements. The step size was adjusted as 0.03. Total measurement time was 20 minutes for every sample. The diameter of goniometer was 310 mm. Type 2 glassy carbon was used as a control before every measurement.

The SAXS data are presented as intensity, I, versus scattering vector, q, where $q=(4\pi/\lambda)\sin\theta$, where 2θ is the radial scattering angle. Average interdomain spacings, which is the average spacing between two repeating hard segments, were calculated with the following formula; $d = (2\pi)/q_{max}$.

2.4.5. Differential Scanning Calorimetry (DSC)

A Model Q100 DSC from TA Instruments with refrigerated cooling system was used. 8-12 mg samples were enclosed in hermetically sealed aluminum pans. All samples, except the PDMS based copolymer samples were cooled down to -100 °C (PDMS based samples were cooled down to -150 °C), equilibrated for 15 minutes and then heated to +200 °C with a heating rate of 10 °C/min. Temperature and enthalpy calibration of the instrument was performed by using standard indium and zinc samples.

2.4.6. X-Ray Photoelectron Spectrometry (XPS)

ThermoScientific K-Alpha X-Ray Photoelectron Spectrometer (XPS) equipped with a monochromatic Al Kα excitation source (1486.6 eV) and hemispherical analyzer was used for surface chemical composition analysis. The spot size of the beam was 400 μm. The take off angle was set at 90°. XPS atomic compositions were collected from a depth of ~10 nm and ratios were determined by using the supplied Avantage software. A flood gun was employed to reduce surface charging and binding energies were referenced to the carbon 1s primary signal at 284.4 eV.

2.4.7. Static Water Contact Angle Measurements

Thin and homogenous polymer films were obtained by using a spin-coating process for water contact angle measurements. 8-10 drops of polymer solutions with a concentration of 5% by weight were spin coated on 20 x 20 mm ISOLAB microscope cover glasses with thicknesses between 0.13-0.17 mm. Specialty Coating Systems Spin Coater® P6700 was used at 1000 rpm for 60 seconds for this purpose. Following this, samples were left under the hood at room temperature for slow evaporation. Polymer coated glass slides were then put in 60 °C air oven for 8 hours and were later on put in vacuum for another 8 hours to ensure complete removal of the solvent.

A 5 μL droplet of deionized, triple distilled water was deposited onto the polymer films by a micro syringe. Static water contact angles at room temperature were measured according to the standard sessile drop method by using a KRÜSS G-10 goniometer fitted with a digital camera. Reported contact angles values are obtained by averaging at least five measurements.

2.5. Biofilm Assays

The biofilm assay experiments were done as a collaborative project with the clinical microbiology laboratory supervised by Prof. Dr. Füsun Can at Koc University. Medical grade PVC was used as the control system since this material is commonly used in medical equipment (such as endotracheal tubes, catheters etc.) associated with problems of biofilm formation.

2.5.1. Materials

Phosphate Buffered Saline (PBS) (10X) was purchased from Thermo Scientific. Bacto Tryptic Soy Broth (TSB) and Difco Tryptic Soy Agar (TSA) was purchased from Becton, Dickinson and Company. *Staphylococcus aureus* 700698 was purchased from ATCC ®.

2.5.2. Procedure

5 Identical circular discs were cut from solvent cast polymer films for the assays. Films had a diameter of 1.0 cm and a thickness of 0.5 to 1.0 mm.

The bacterium was incubated overnight at 37 °C and its concentration was measured using a densitometer. The concentration of the bacterium is set to 1.0 at McFarland Standarts. Previously prepared TSB solution (30gr/L) with a 1% by weight glucose content was put in a test tube. The bacterium was added on this medium to give a final concentration of 1 mcF. 40 mL of this inoculum was further diluted 10 times by adding 360 mL sterile TSB solution with a 1% wt glucose content. This new inoculums was distributed to 5 test tubes because the same experiment was performed to 5 different discs of the same polymer. 25 mL of inoculum was put in each of these test tubes. A single polymer disc was put in each tube and all tubes were put in 37 °C incubator for 24 hrs. After incubation, the liquid inside the test tubes were sucked out with the help of a pipette and 25 mL of fresh PBS solution prepared with distilled water (1X) was poured inside each test tube. The test tubes were manually shaken in order to get rid of the bacterium that are not part of the biofilm. These discs were then taken out with the help of tweezers and put in 10 mL of fresh PBS solution (1X) and they were first subjected to vortex for 5 minutes at 2200 rpm and secondly sonicated for 1 minute at 40 Hz. The PBS solution (1X) now contains the bacterium that was part of the biofilm. This solution was diluted 6 times, each time being diluted for 10 fold. From each of these 6 dilutions 100 µL of bacterium sample was inoculated on an agar plate (prepared with 40gr/L TSA dolution prepared with distilled water and autoclaved) and 3 agar plates were prepared from each dilution. These agar plates were then incubated overnight at 37C ° for 24 hours and colony count was performed.

CHAPTER 3

RESULTS AND DISCUSSIONS

This study comprises of synthesis and characterization of TPUUs based on five different polyethers in order to investigate their structure-morphology-property relationships. This work is a continuation of numerous studies conducted by Yilgör Polymer Research Group investigating the structure-morphology-property relationships in segmented TPUUs. Due to their interesting combination of surface and bulk properties, which provide them with blood and tissue compatibility, TPUUs hold the potential of being used as biomaterials. The main goals of this study were the investigation of the influence of:

(i) soft segment structure,
(ii) soft segment molecular weight, and
(iii) hard segment content on the copolymer morphology, bulk and surface properties.

In addition, influence of the surface composition and surface energy of the TPUU films on biofilm formation was also investigated.

3.1 Structural design and synthesis of TPUUs

Five different soft segments (SS) used for this study included poly(ethylene oxide) glycol (PEO), poly(propylene oxide) glycol (PPO), poly(tetramethylene oxide) glycol (PTMO), amine and hydroxyl terminated polydimethylsiloxane (PDMS) and a polyfluoroether (PFE) (Fluorolink E10-H®). Two different molecular weights of each SS were used except for the PFE, which was synthesized from E10-H® (Mw=1,400 g/mol). The molecular weights of poly(ethylene oxide), poly(propylene oxide) and poly(tetramethylene oxide) used were 1,000 and 2,000 g/mol. The molecular weights of the amine and hydroxyl terminated PDMS were varied as 900 and 2500 g/mol. The HS contents of the PUUs were usually kept constant at 20 and 30% by weight. There were some exceptional cases when the HS contents were 16 and 25% by weight.

Due to their exceptional resistance to solubility in common organic solvents, it is challenging to synthesis PFE based copolymers with high HS contents. Therefore *non-chain extended* PFE based copolymers resulting in 16% wt of HS and chain extended PFE based copolymers

resulting in 20% wt HS were synthesized for studying the effect of increasing HS content in these copolymers.

Non-chain extended TPU obtained by the stoichiometric reaction of PTMO-1K and HMDI yields a copolymer with about 22% by wt HS content. This copolymer forms a sticky film with no mechanical integrity [14], therefore PTMO1-UU-25 was synthesized for comparison purposes.

The list of copolymers synthesized for this study, together with their detailed compositional descriptions is provided in Table 2.2. As mentioned in Chapter 2, all copolymers were synthesized using the two-step "prepolymer" method except the *non-chain extended* polymers, which were synthesized in a single step. During the chain extension step overall molecular weight of the copolymer chains increase while highly polar urea or urethane groups are introduced into their backbones. The strong hydrogen bonding capacity of the urea or urethane linkages can cause physical gelation during the chain extension step. When the chains are in close contact, physical 3D network structures can be born and the polymer chains can get locked making it impossible to further increase the molecular weight of the copolymers. [62] In order to prevent this problem, highly polar solvents such as IPA or DMF are used to dilute the polymer solution during synthesis when viscosity increases.

The approach used in copolymer coding or nomenclature has already been discussed in Chapter 2. For example a PEO-2K based PUU with a hard segment content of 30% by weight is coded as: PEO2-UU-30.

As clearly described in Chapter 2, the polymerization reactions were followed by FT-IR spectroscopy. As a general example, the spectra obtained during various reaction stages for the synthesis of PTMO2-UU-30 are presented in Figure 3.1.

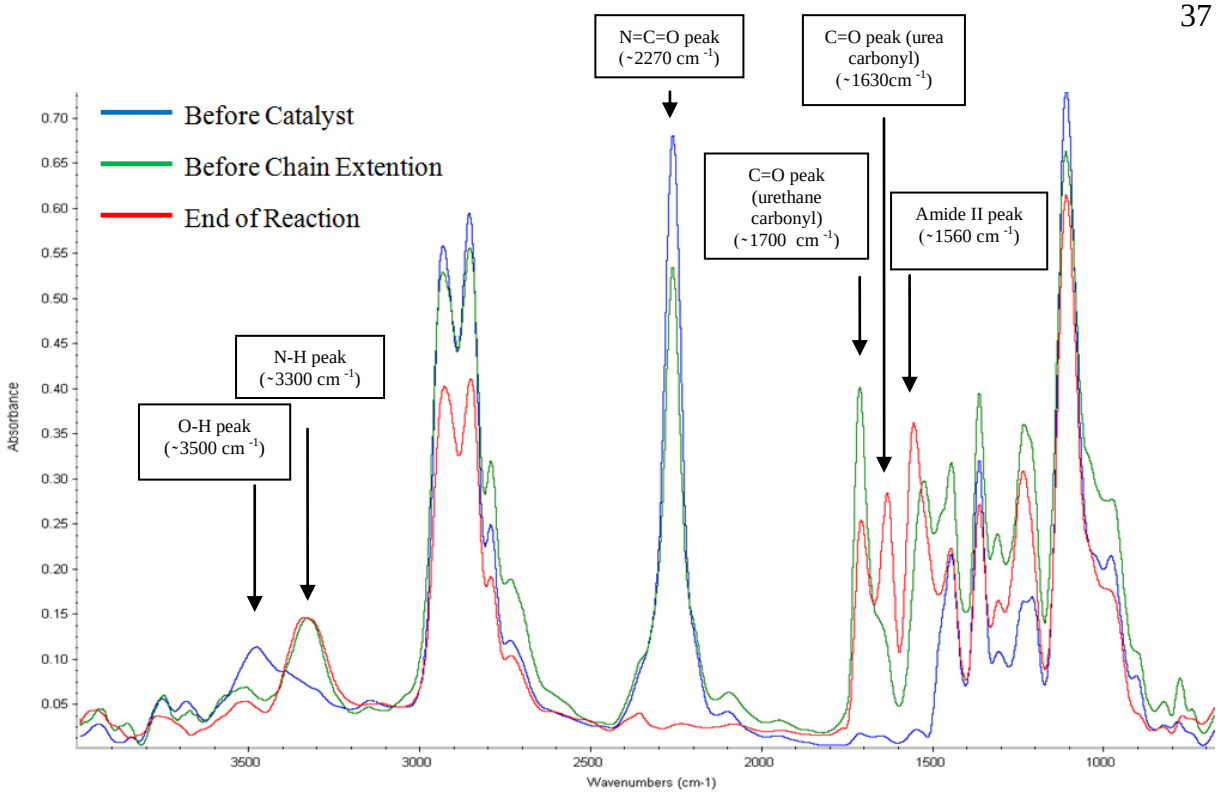

Figure 3.1. FT-IR spectra of the reaction mixture at various stages during the PTMO2-UU-30 synthesis.

The blue curve was taken immediately after mixing the PTMO and HMDI in the reactor for the preparation of the prepolymer. The hydroxyl ends of the PTMO give a strong and broad peak centered around 3500 cm^{-1} and the isocyanate from the HMDI gives a very strong and sharp peak at 2270 cm^{-1}. As the reaction proceeds and prepolymer starts forming, the hydroxyl and the isocyanate peaks gradually decrease, while a urethane N─H peak is formed around 3300 cm^{-1} as seen in the green curve. A very strong urethane carbonyl peak around 1700 cm^{-1} has also formed at this point. As chain extension takes place, all the isocyanate reacts with the amine groups from MDAP leading to the complete elimination of the isocyanate peak and the formation of the urea carbonyl peaks around 1630 cm^{-1} as clearly observed in the red curve. An amide II peak is also observed at 1550 cm^{-1} as polymerization comes to an end. The amide II peak has a complex structure mainly affected by the C-N stretch and C-N-H bending modes. [64] It is a mixed vibration that is sensitive to conformation via mechanical coupling and hydrogen bonding. [65]

3.2.1. ATR-FTIR Analysis of the Hydrogen Bonding in the Carbonyl Groups

As discussed in detail in Chapter 1, one of the most important factors affecting the microphase separation in segmented PUUs is the ability and strength of hydrogen bonding within the urethane or urea HS. Infrared spectroscopy is a simple yet powerful technique to characterize the degree of hydrogen bonding in carbonyl compounds. [13]

The presence of hydrogen bonding disturbs the vibrational motions of the functional groups, which results in a shift of peak positions to lower frequencies. Peak positions of hydrogen bonded and free urethane and urea carbonyls are given in Table 3.1. It has been proposed that N─H stretching regions do not give reliable results for quantitative analyses due to the fact that N─H groups can hydrogen bond with soft segment ether oxygen as well as the hard segment carbonyls. [65] On the other hand, the carbonyl regions of urethane and urea have been widely studied to understand the degree of microphase separation. [13] If an N─H group hydrogen bonds with an ether oxygen resulting in phase mixing, a carbonyl group from urethane (or urea) is liberated. Therefore the state of the carbonyl groups is a good representation of the nano structure of the polymer. The nature as well as the extent of hydrogen bonding can be characterized by studying the carbonyl regions. Thus the carbonyl regions of the PUUs are discussed in this study.

Table 3.1. Characteristic IR Absorption Frequencies of TPU and PU. [44]

Group	Mode	Frequency (cm^{-1})
C=O (urethane)	Free	1730-1740
C=O (urethane)	C=O···N-H	1703-1710
C=O (urea)	Free	1690-1700
C=O (urea)	C=O···N-H	1660-1670 (disordered)
C=O (urea)	C=O···N-H	1630-1645 (ordered)

The ATR-FTIR carbonyl regions (1600-1800 cm^{-1}) of polymers will be presented in this thesis to investigate the extent and nature of the hydrogen bonding in copolymers at their

equilibrium morphologies. Hydrogen bonding in copolymers with different SS of similar average molecular weights and hard segment contents will be compared in order to understand the morphological differences between them qualitatively.

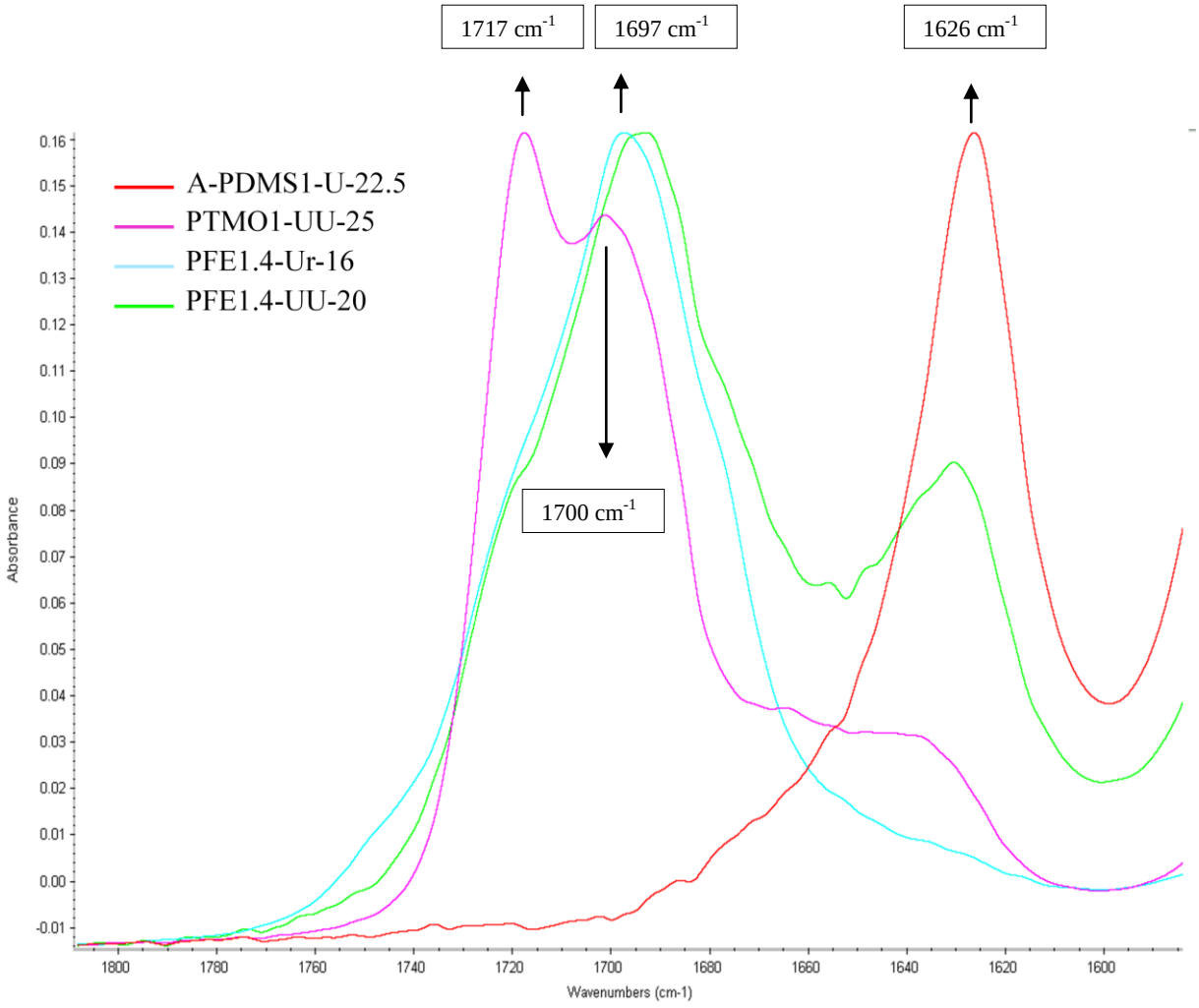

Figure 3.2. ATR-FTIR spectra of polymers with soft segments of 1000 and 1400 g/mol average molecular weights and with hard segment contents of 16, 20 and 25 % by weight.

The ATR-FTIR spectra of the carbonyl region of A-PDMS1-U-22.5, PTMO1-UU-25, PFE1.4-Ur-16 and PFE1.4-UU-20 are reproduced in Figure 3.2. As stated in section 3.1, due to their exceptional resistance to solubility in common organic solvents, it is challenging to synthesize PFE based copolymers with high HS contents, especially when the HS is urea. Therefore, *non-chain extended* PFE based TPU resulting in 16% wt of HS and MDAP chain

extended PFE based PUU resulting in 20% wt HS were synthesized in order to investigate the effect of increasing HS content on the morphology and properties of these copolymers. *Non-chain extended* TPU obtained by the stoichiometric reaction of PTMO-1K and HMDI yields a copolymer with about 22% by wt HS content. This copolymer forms as a sticky film with no mechanical integrity [14], therefore PTMO1-UU-25 was synthesized for comparison purposes. A-PDMS1-U-22.5 was not chain extended in order to get a polymer with a HS content close to 20%wt.

When the FTIR spectra provided in Figure 3.2 are closely examined it can easily be seen that silicone-urea copolymer (A-PDMS1-U-22.5) displays a single, sharp absorption peak centered at 1626 cm^{-1}, which indicates strongly hydrogen bonded and ordered urea carbonyls. This is expected since PDMS based copolymers show excellent microphase separation due to the dramatic solubility differences between PDMS (15.6 $(J/cm^3)^{1/2}$) and urea groups (45.6 $(J/cm^3)^{1/2}$). A-PDMS is an amine terminated oligomer, therefore results in pure urea linkages when reacted with isocyanate. This sample was not chain extended.

Interestingly, when the FTIR spectrum of PTMO1-UU-25, which is a PUU, is closely examined, three well-defined peaks in the carbonyl region centered at 1717, 1700 and 1637 cm^{-1} can readily be identified. The strong absorption peak with a peak maximum at 1717 cm^{-1} is an indication of the presence of weakly hydrogen bonded urethane groups, as already shown by our group on PEO and PPO based PUUs [10]. This is mainly due to the presence of competitive urethane-ether interactions, which weakens the urethane-urethane interactions and leads to microphase mixing in these copolymers. The second strong peak at 1700 cm^{-1} is most probably due to a combination of ordered hydrogen bonded urethane and free urea carbonyls. In addition, since PTMO1-UU-25 contains a very small amount of chain extender to obtain 25% by wt hard segment content, a weaker absorption band at 1637 cm^{-1} indicates the presence of ordered hydrogen bonded urea peak when compared with the other copolymers.

Yilgor and co-workers have shown that urethane carbonyls forming medium to strong hydrogen bonding with a HMDI HS show a peak maximum at 1695 cm^{-1} and urethane carbonyls forming well ordered strong hydrogen bonding show a peak maximum at 1685 cm^{-1} [13]. When the carbonyl region of the PFE1.4-UU-20 spectrum is examined, similar to PTMO1-UU-25 three distinct carbonyl absorptions are observed. However, due to major differences between the backbone structures of PTMO and PFE, the shapes and the positions

of the peaks are remarkably different. A strong shoulder at 1717 cm^{-1} indicates the presence of weakly hydrogen bonded urethane groups. A very strong peak at 1694 cm^{-1} clearly shows the presence of strongly hydrogen bonded urethane groups. In addition a well-defined and strong absorption peak at 1635 cm^{-1} also shows the presence of strongly hydrogen bonded urea hard segments. When the spectra for PTMO and PFE based PUUs are compared, it can easily be seen that in PFE based PUU both urethane and urea hard segments can form stronger hydrogen bonding when compared with that of PTMO based copolymer. This also indicates a much better microphase separation in PFE based PUU. This is expected since the ether oxygen in PFE is somewhat protected by the fluoromethyl groups and cannot easily interact with the N─H groups. In addition due to very strong electronegativity of the fluorine atoms, the ether oxygen in PFE is more electropositive than that of PTMO, which also weakens the possible interaction with the urethane or urea groups.

PFE1.4-Ur-16 is a *non-chain extended* TPU obtained by stoichiometric reaction of HMDI and PFE1.4. Since the oligomer was hydroxyl terminated, this polymer resulted in urethane linkages with uniform lengths. PFE1.4-Ur-16's urethane peak maximum is at 1697 cm^{-1} indicating medium to strong hydrogen bonded urethane groups. It has stronger hydrogen bonded urethane groups compared to PTMO based PUU. Similar to PFE1.4-UU-20 PFE1.4-Ur-16 also has a broad shoulder around 1715 cm^{-1} indicating also the presence of small amounts of weakly hydrogen bonded urethane groups.

In order to understand the effect of hard segment content on the nature and extent of hydrogen bonding in these segmented TPU and PUU copolymers the ATR-FTIR spectra of the carbonyl region of A-PDMS1-U-30, H-PDMS1-Ur-30, PEO1-UU-30, PPO1-UU-30 and PTMO1-UU-30 are provided in Figure 3.3.

Similar to A-PDMS1-U-22.5, there is only a single absorption peak centered at 1625 cm^{-1} in the FTIR spectrum of A-PDMS1-U-30, confirming the existence of only ordered and strongly hydrogen bonded urea carbonyls in the copolymer. Similar to A-PDMS1-U-22.5 this clearly indicates excellent microphase separation for this sample, which is expected.

For comparison, FTIR spectrum of a siloxane-urethane H-PDMS1-Ur-30 is also provided. The peak maximum of H-PDMS1-Ur-30 is at 1695 cm^{-1} confirming the existence of medium to strong hydrogen bonding between the urethane HS. The peak maximum is skewed to the right towards 1685 cm^{-1} confirming the dominance of well ordered strong hydrogen bonding.

However the broad shoulder centered at 1712 cm^{-1} also indicates the presence of weakly hydrogen bonded urethane groups.

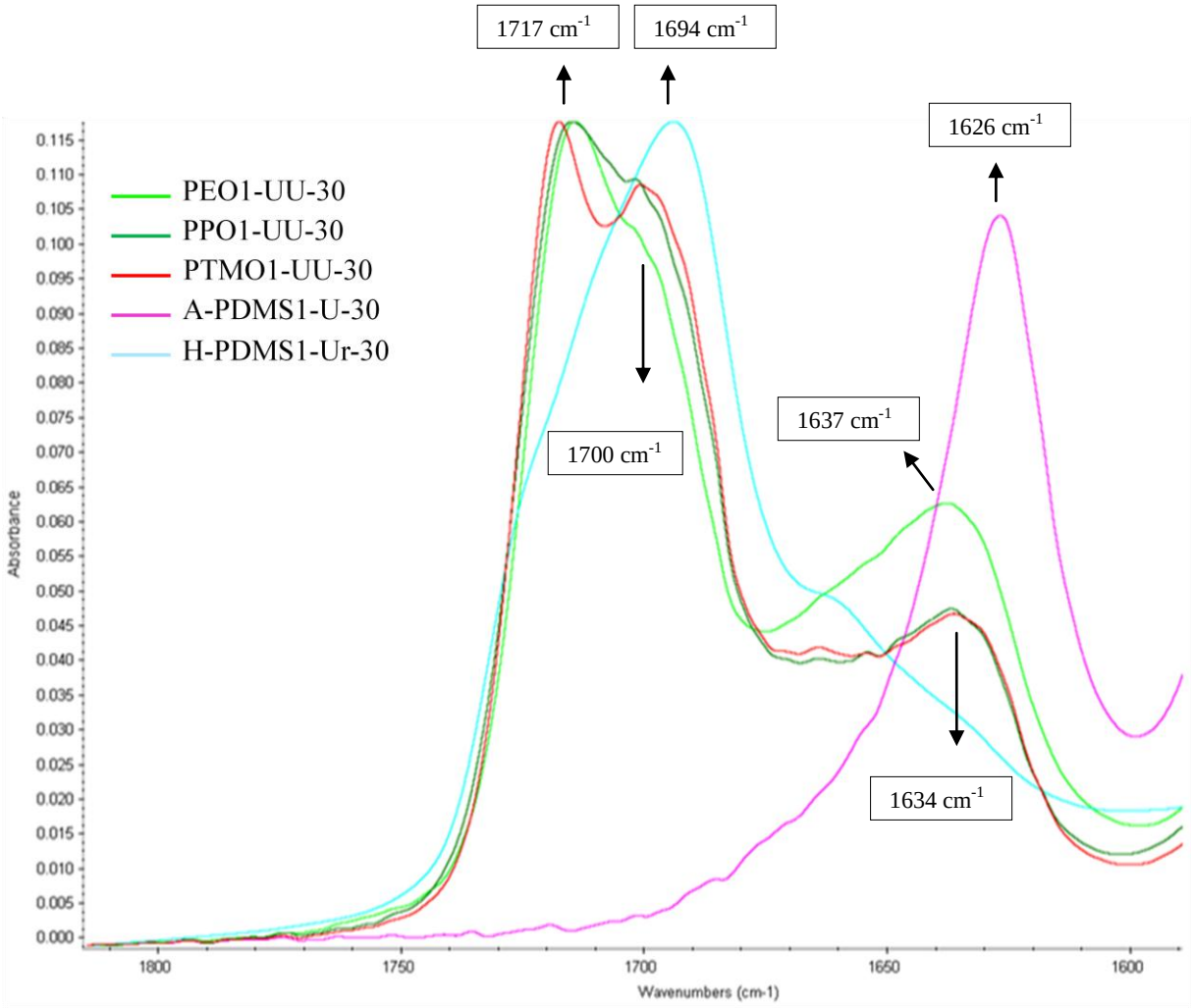

Figure3.3. ATR-FTIR spectra of polymers with soft segments of 1000 g/mol number average molecular weights with 30 % weight hard segments.

The polyether based PUUs, regardless of the actual structure of the soft segment (PEO, PPO or PTMO) all show fairly strong peaks in the weakly hydrogen bonded urethane region of 1717 cm^{-1}. This indicates that phase mixing exists in all polyether based polymers. All three polyether based PUU also show peaks in the 1700 cm^{-1} region. This region is a combination of ordered hydrogen bonded urethane group peaks with free urea group peaks, therefore it is not possible to make a comparison between the phase organizations of polyethers based on these regions. Very interestingly, PEO based PUU has an ordered hydrogen bonded urea peak

with a maximum at 1637 cm^{-1} whereas the ordered hydrogen bonded urea peaks of PPO and PTMO based PUU have a maximum at 1634 cm^{-1}. It must be noted that the urea peak of A-PDMS based PUU is in much lower frequencies (1626 cm^{-1}) when compared with polyether based urea peaks indicating the strongest hydrogen bonded urea groups among all polymers investigated in this study.

In addition to the effect of SS structure and HS content, we also investigated the influence of SS molecular weight on the nature and extent of hydrogen bonding in polyether and PDMS based copolymers. The carbonyl region of the ATR-FTIR spectra for A-PDMS2.5-U-20, H-PDMS2.5-Ur-20, PEO2-UU-20, PPO2-UU-20 and PTMO2-UU-20 are reproduced in Figure 3.4.

Similar to the previous results, A-PDMS1-U-30 gives a single peak at 1629 cm^{-1} confirming the existence of well-ordered and strongly hydrogen bonded urea carbonyl groups as expected.

As can be seen from Figure 3.4., H-PDMS2.5-Ur-20 shows three distinct peaks with maxima at 1715, 1695 and 1663 cm^{-1}. The peak at 1715 cm^{-1} indicates the existence of weakly hydrogen bonded urethane groups. The peak maximum at 1695 cm^{-1} indicates the dominance of medium to strong hydrogen bonding in its urethane groups. The shoulder observed at 1663 cm^{-1} for H-PDMS1-Ur-30 has now clearly become a distinctive peak for H-PDMS2.5-Ur-20. Even though H-PDMS2.5-Ur-20 has a lower HS content than H-PDMS1-Ur-30, the fact that it is based on a higher molecular weight oligomer provides H-PDMS2.5-Ur-20 with stronger hydrogen bonded urethane groups. This clearly demonstrates the strong influence of PDMS molecular weight on microphase separation in silicone-urethane copolymers.

The polyether based TPUs all show broad peaks in the region of weakly hydrogen bonded urethane groups (1717 cm^{-1}). PEO2-UU-20 especially shows a peak at 1752 cm^{-1} confirming the existence of non-hydrogen bonded, or free carbonyl groups in its structure. This happens when a hydrogen from the amine group hydrogen bonds with an oxygen from an ether liberating a carbonyl from the urethane group. This is expected since PEO has the highest concentration of ether oxygens in its backbone when compared with PPO and PTMO. In addition PEO also has the highest solubility parameter (20.2 $(J/cm^3)^{1/2}$) when compared with PPO (18.9 $(J/cm^3)^{1/2}$) and PTMO (17.6 $(J/cm^3)^{1/2}$), therefore is expected to have the highest

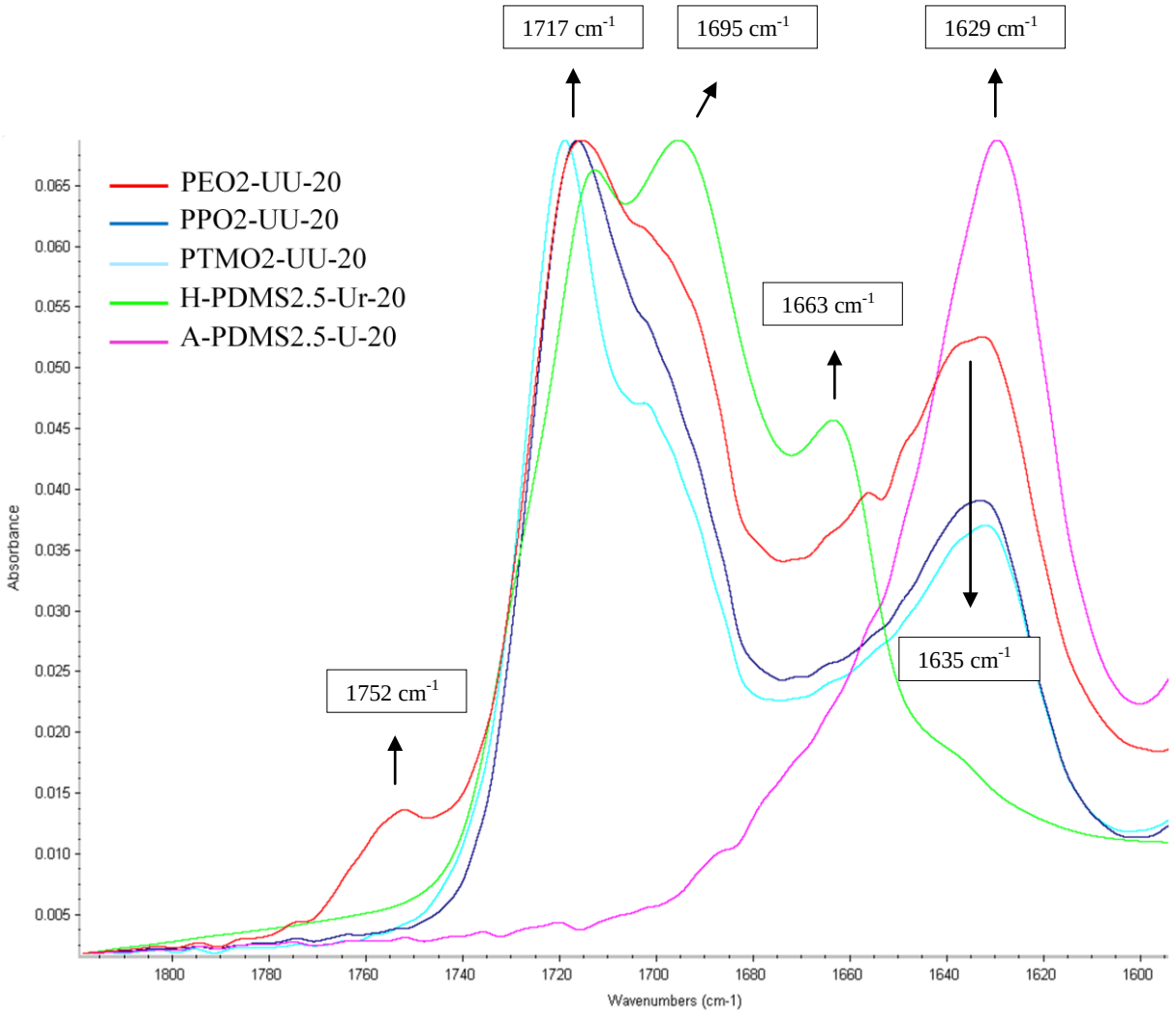

Figure 3.4. ATR-FTIR spectra of polymers with soft segments of 2000 and 2500 g/mol average molecular weights and with 20% by weight hard segment contents

amount of phase mixing. Polyether based PUUs all have shoulders around 1700 cm^{-1}which is a combination of hydrogen bonded urethane groups and free urea groups. Very interestingly, PEO based PUU also has the strongest peak at 1635 cm^{-1}, which shows the presence of strongly hydrogen bonded urea groups. This may only be due to the crystallization of the PEO soft segments in the copolymer, which allows a better network formation between the urea groups. In fact, as will be discussed later on in tensile properties, PEO2-UU-20 gives a fairly brittle and fragile film.

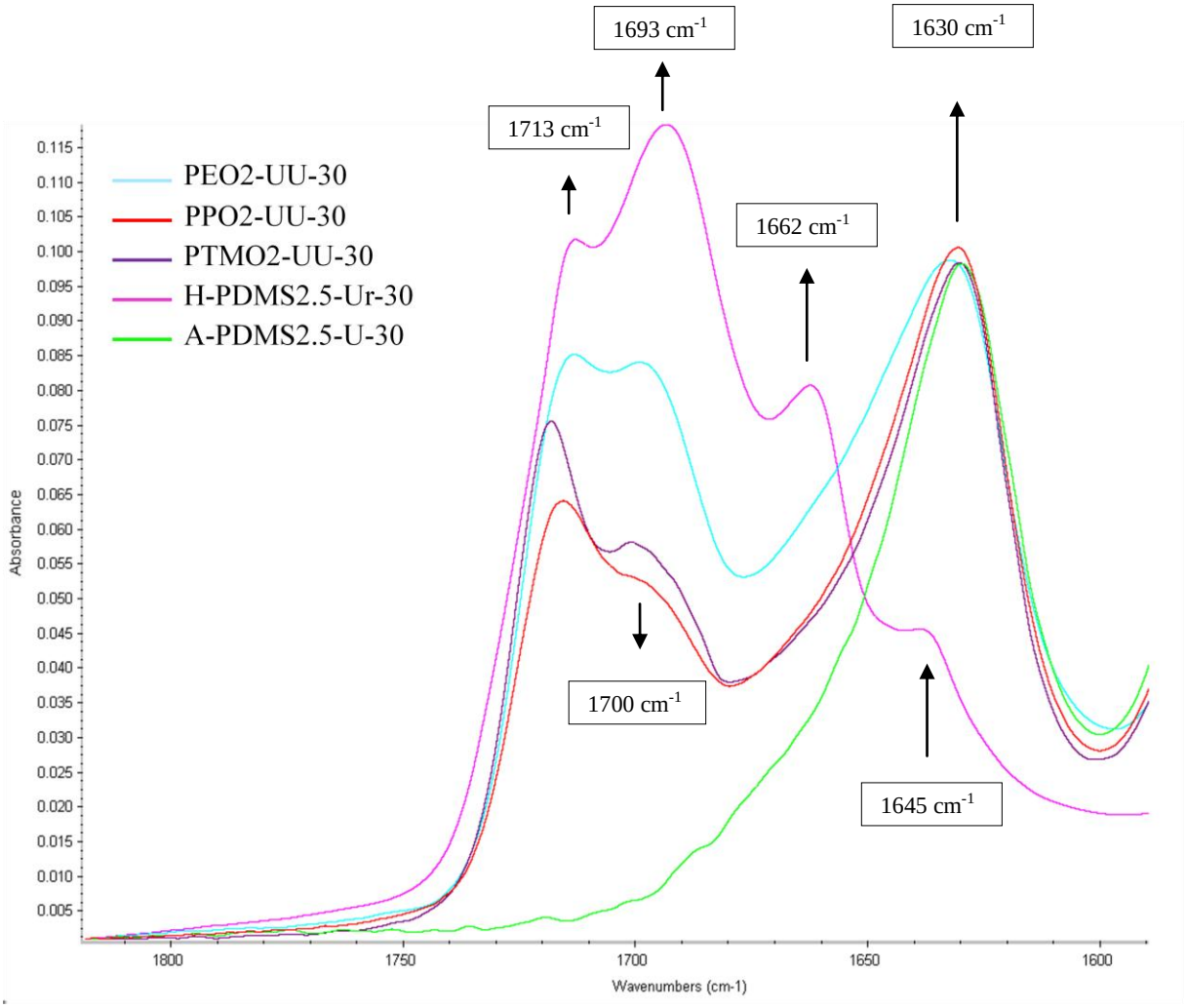

Figure 3.5. ATR-FTIR spectra of TPUU copolymers with soft segments of 2000 and 2500 g/mol average molecular weights with 30% by wt hard segment contents.

Finally in order to understand the effect of higher molecular weight SS and higher HS content on the nature and extent of hydrogen bonding in the carbonyl region, ATR-FTIR spectra were also obtained. FTIR spectra of A-PDMS2.5-U-30, H-PDMS2.5-Ur-30, PEO2-UU-30, PPO2-UU-30 and PTMO2-UU-30 are reproduced in Figure 3.5.

Very similar to observations made on copolymers with different PDMS molecular weights and/or HS contents, A-PDMS2.5-U-30 shows a single, strong peak centered at 1631 cm^{-1} again indicating presence of very strong and ordered hydrogen bonding between urea groups. As already indicated before, due to dramatic differences between the polarities or solubility parameters of PDMS and urea groups regardless of the SS length (1000 or 2500 g/mol) or HS

content (20 to 30% by weight) they always display excellent microphase separation, which is clearly indicated by a single strongly hydrogen carbonyl peak around 1630 cm^{-1}.

Carbonyl region of the FTIR spectrum for H-PDMS2.5-Ur-30 copolymer shows four distinct absorption peaks with maxima at 1713, 1693, 1662 and 1645 cm^{-1}. 1693 cm^{-1} peak shows the dominance of medium to strongly hydrogen bonded carbonyl groups, while the peak at 1662 cm^{-1} is possibly an indication of well-ordered and hydrogen bonded urethane groups. The peak at 1662 cm^{-1} only existed as a small shoulder in H-PDMS1-Ur-30, however it exists as distinct peaks both for H-PDMS2.5-Ur-20 and H-PDMS2.5-Ur-30. In addition H-PDMS2.5-Ur-30 also shows a well-defined absorption peak at 1645 cm^{-1}, which indicates the presence of strongly hydrogen bonded and well-ordered urethane HS. These results demonstrate that stronger hydrogen bonding within urethane HS in silicone based TPUs with higher molecular weight SS oligomers lead to improved microphase separation.

The broad carbonyl peaks observed around 1715 cm^{-1} in polyether based PUUs, which indicate presence of weakly hydrogen bonded urethane groups again suggest existence of phase mixing in these copolymers. Also all polyether based PUUs show shoulders around 1700 cm^{-1} which is a region for hydrogen bonded urethane groups and/or free urea groups. As expected, strongly hydrogen bonded urea peaks around 1630 cm^{-1} are all stronger for copolymers containing 30% by weight hard segments.

When comparing all PUUs, only PDMS and PFE based polymers show medium to strong hydrogen bonded urethane groups around 1695 cm^{-1}, while the polyether based copolymers show fairly large amounts of disordered hydrogen bonded urethane groups (~1717 cm^{-1}). This is expected since PDMS (15.6 $(J/cm^3)^{1/2}$) and PFE (<15 $(J/cm^3)^{1/2}$) have lower solubility parameters compared to PEO (20.2 $(J/cm^3)^{1/2}$), PPO (18.9 $(J/cm^3)^{1/2}$) and PTMO (17.6 $(J/cm^3)^{1/2}$) resulting in better microphase separated morphologies.

It is also interesting to observe that PDMS and PFE based TPUs have broad urethane carbonyl peaks indicating the existence of hydrogen bonded urethane carbonyls in various forms including the ordered and disordered forms, whereas the PDMS based PU copolymers only show a single urea carbonyl peak indicating the presence of only well ordered hydrogen bonded urea carbonyls. This is expected due to the nature of the hydrogen bonding between urea groups which form bidentate hydrogen bonds as shown in Figure 1.13, whereas the urethane groups can only form monodentate hydrogen bonds. Therefore copolymers with urea linkages tend to better microphase separate when compared with their urethane analogs. It has

previously been demonstrated by Yilgor et.al. that *non-chain extended* TPU systems that do not have any mechanical integrity at room temperature, do form strong films at room temperature when the urethane linkages are replaced with urea linkages. [14]

3.3. DSC Analysis

Differential scanning calorimetry (DSC) is a very simple and powerful technique, which provides very useful supporting information on the microphase morphologies of block and segmented copolymers. It is possible to determine the glass transition temperatures (T_g), and crystallization (T_c) and melting (T_m) points and enthalpies of polymers/copolymers by DSC. In block or segmented copolymers generally presence of two separate T_g values indicate a microphase separated morphology. Comparison of the T_g values of each segment obtained in a block or segmented copolymer with those of pure homopolymers also may provide valuable information on the extent of phase mixing.

As a general example to demonstrate the use of DSC measurements in TPUs, low temperature (-90 to +50 °C) DSC thermogram of PEO2-UU-30 is provided in Figure 3.6.

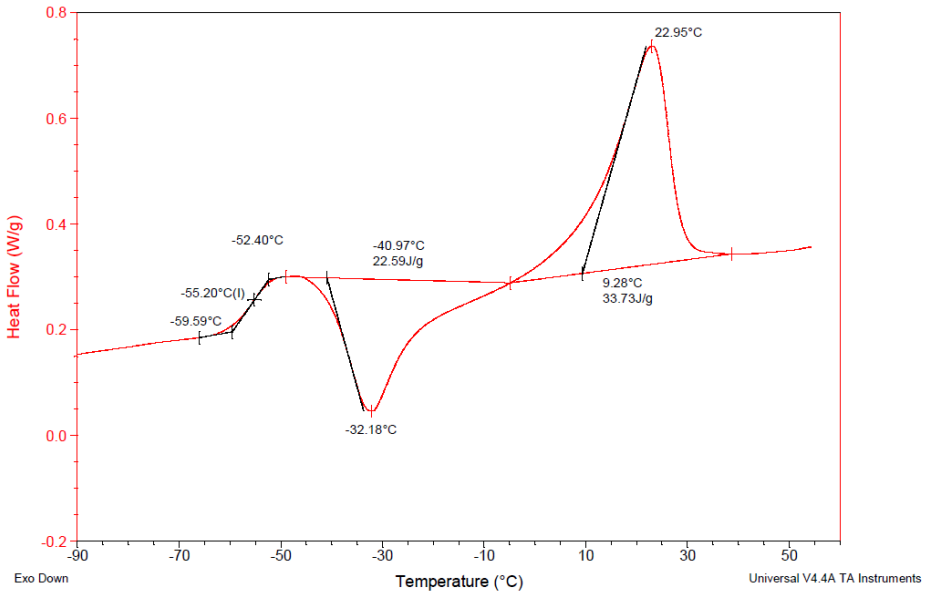

Figure 3.6. DSC thermogram of PEO2-UU-30.

As can be seen from this figure, PEO2-UU-30 displays a PEO SS T_g at -55.2 °C, a broad PEO crystallization peak ranging from -35 to about 0 °C, with a maximum at -32.18 °C and a broad melting peak in 0 to 35 °C range, with a peak maximum of 22.95 °C. Enthalpy of crystallization and melting, which can be calculated from the peak areas are obtained as 22.59 and 33.73 J/g respectively indicating that the copolymer was partially crystalline before the DSC measurements were made. All these results clearly indicate that PEO2-UU-30 has a microphase separated morphology, which clearly supports the observations made in FTIR studies. The T_g value for pure PEO-2000 is given as -60 °C in the literature [66], which is very close to the value observed for the PEO2-UU-30 clearly indicating the presence of a fairly pure PEO SS matrix.

DSC thermogram for PEO1-UU-30 is provided in Figure 3.7. As can be seen in this figure there is a sharp glass transition with a T_g value of -47.82 °C for PEO-1000 matrix but no crystallization or melting is observed, typical for low molecular weight PEO oligomers in segmented copolymers. T_g value for PEO-1000 is slightly higher than that of PEO-2000, which is expected.

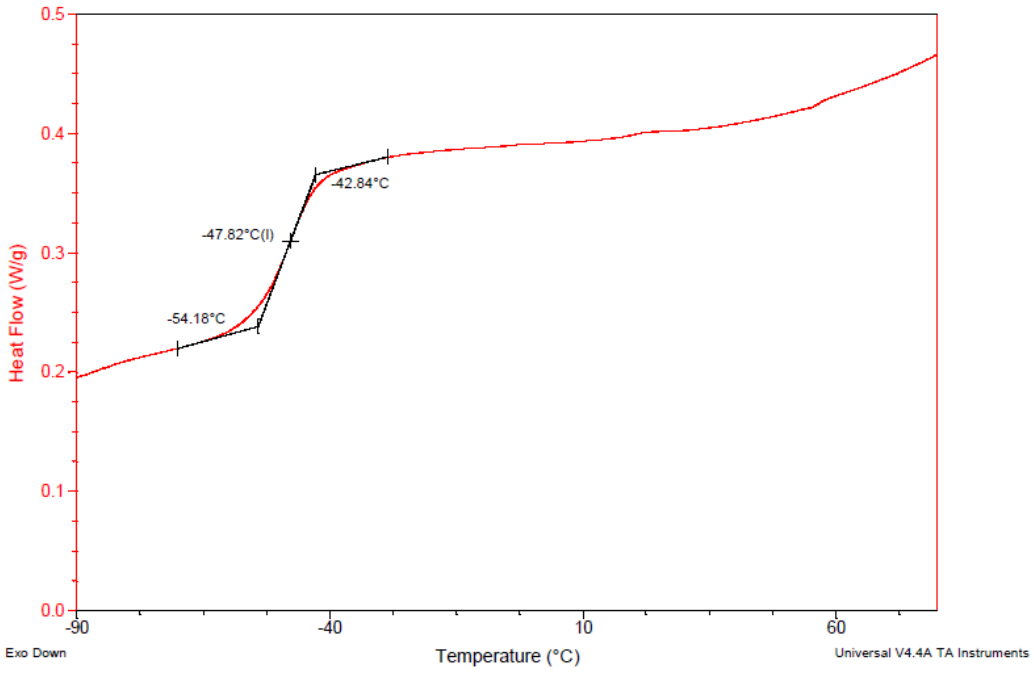

Figure 3.7. DSC thermogram of PEO1-UU-30.

DSC thermograms of various copolymers synthesized and characterized in this study are provided in Figures 3.8 to 3.14. DSC data obtained from these thermograms are summarized in Table 3.3.

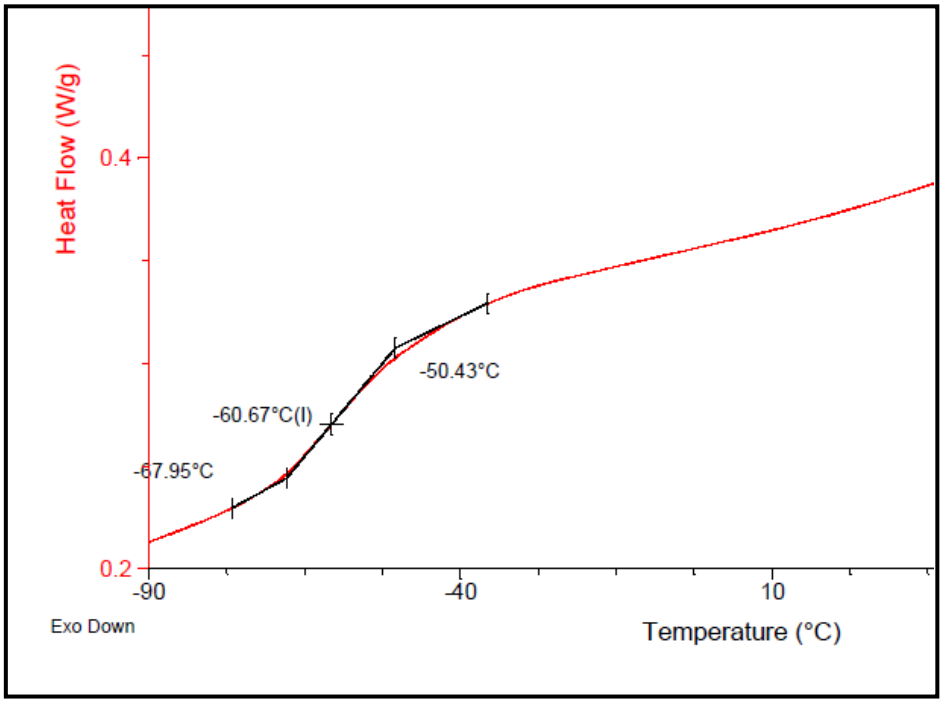

Figure 3.8. DSC thermogram of PTMO1-UU-30.

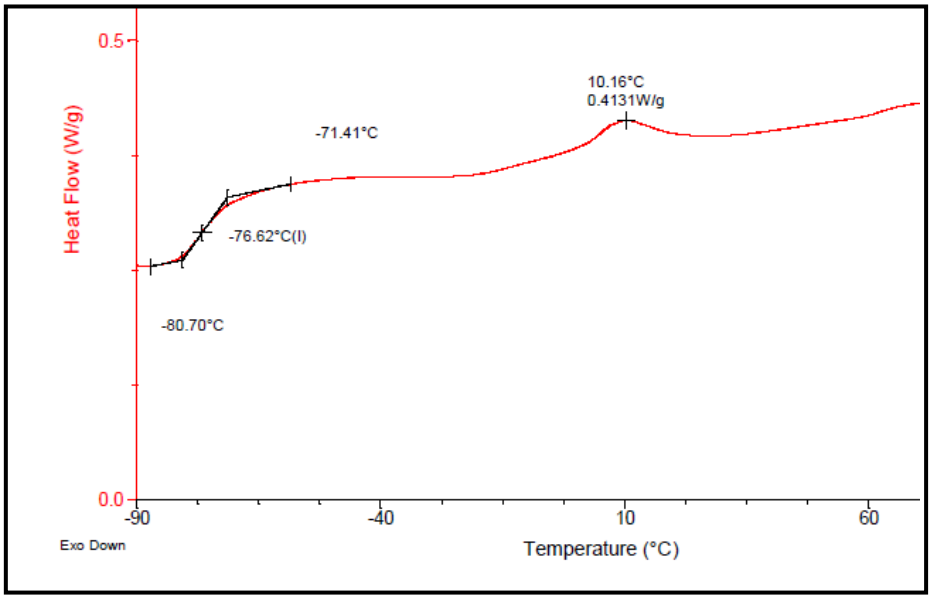

Figure 3.9. DSC thermogram of PTMO2-UU-20.

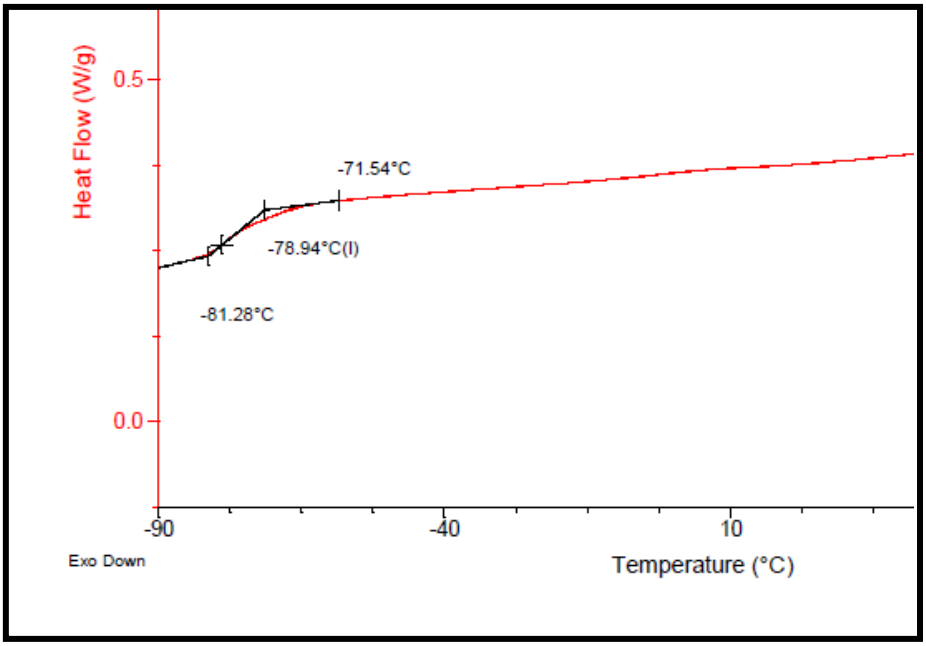

Figure 3.10. DSC thermogram of PTMO2-UU-30.

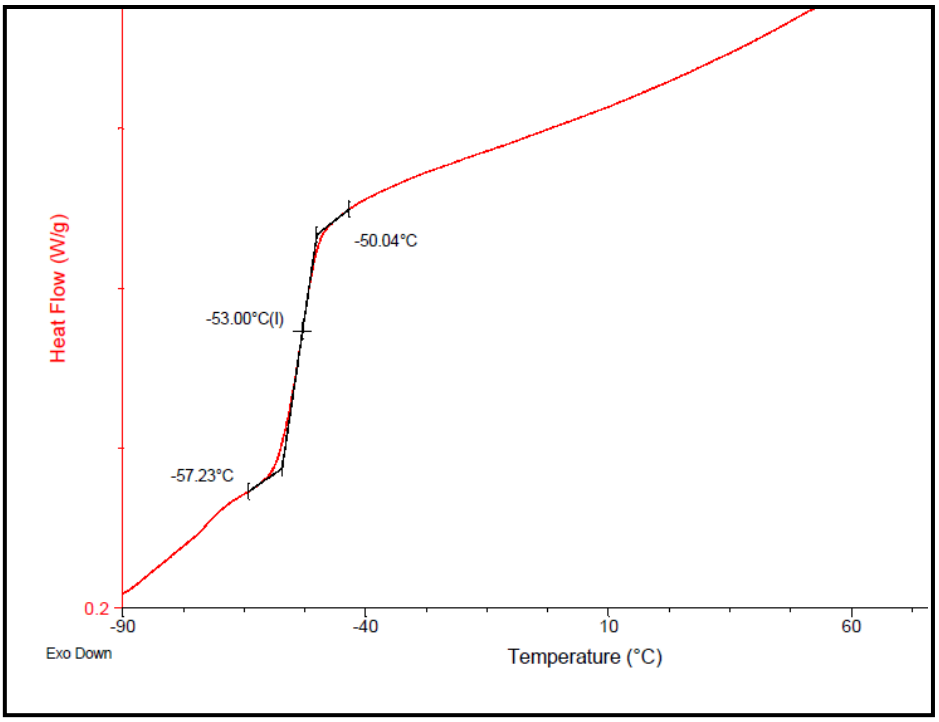

Figure 3.11. DSC thermogram of PPO2-UU-20.

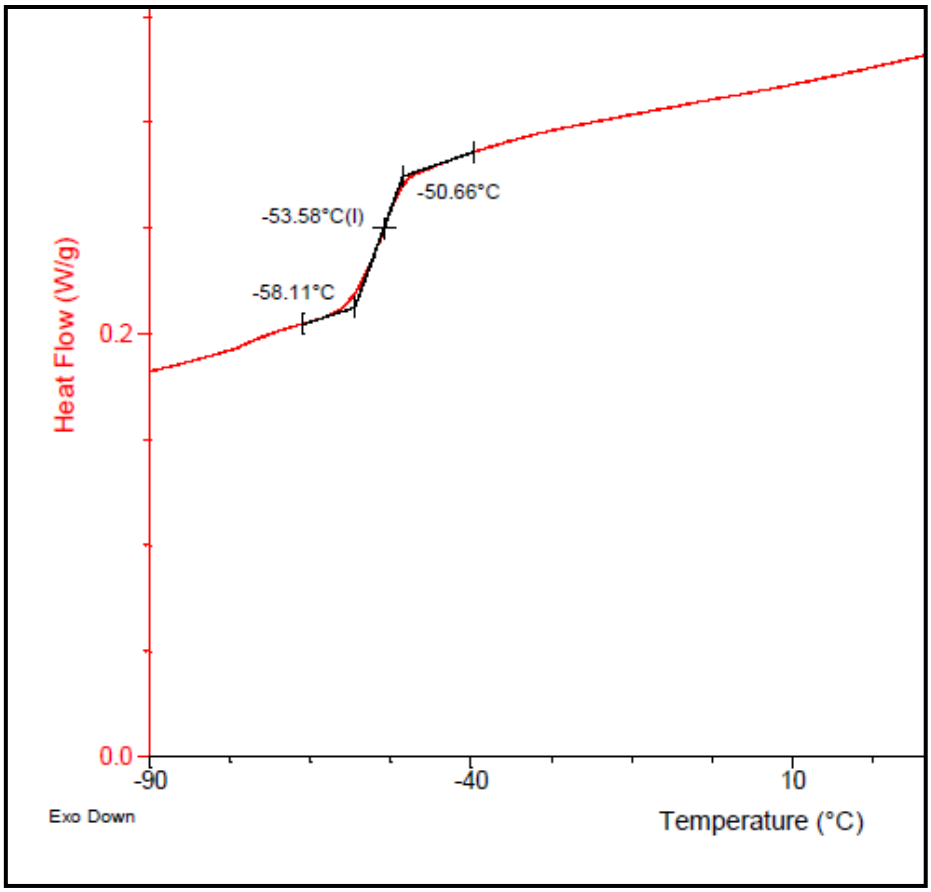

Figure 3.12. DSC thermogram of PPO2-UU-30.

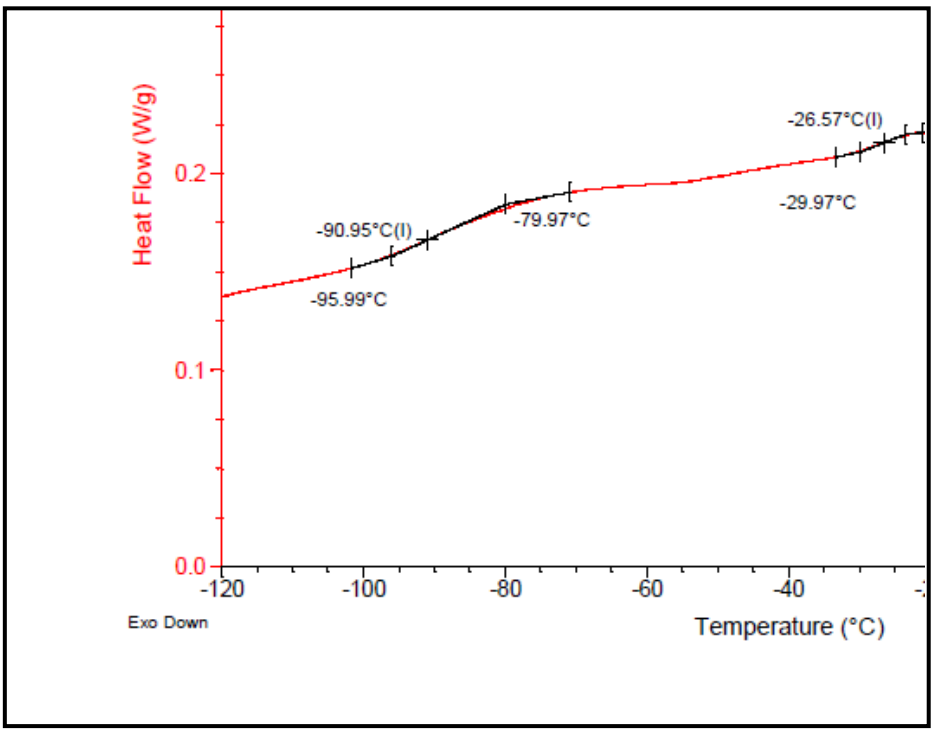

Figure 3.13. DSC thermogram of PFE1.4-Ur-16.

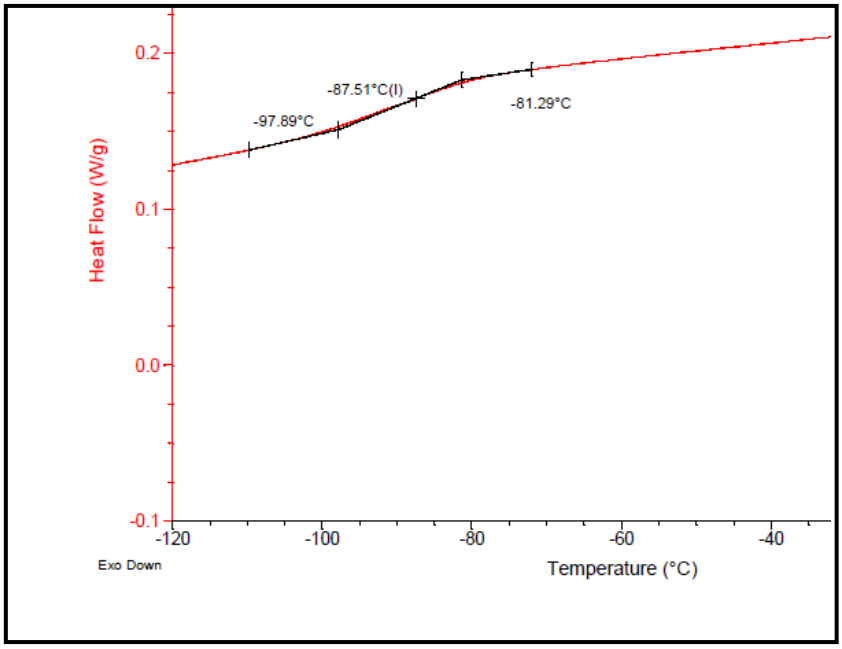

Figure 3.14. DSC thermogram of PFE1.4-UU-20.

The T_g of PTMO is given as -85 °C, PPO as -82 °C and E10-H® as -100 °C in the literature. [25, 67] All copolymers show T_g values close to the pure SS oligomers they are based on, indicating the existence of microphase separation for all, with some variations in degrees. PFE based copolymers show the closest values to their literature value indicating excellent microphase separation. PTMO1-UU-30 shows a T_g higher than its 2K analogs, which is expected, possibly also indicating a more phase mixed system. Copolymers based on PPO with the same SS oligomer $<M_n>$ but different HS shows very similar Tg's around -53 °C, however very interestingly they show fairly large deviations from the literature value of -82 C, which may be an indication of phase mixing in these copolymers.

Table 3.2. Summary of sub-ambient DSC data.

Copolymer	Sub-ambient T_g (°C)
PEO1-UU-30	-47.8
PEO2-UU-30	-55.2
PTMO1-UU-30	-60.7
PTMO2-UU-20	-76.6
PTMO2-UU-30	-78.9
PPO2-UU-20	-53.0
PPO2-UU-30	-53.6
PFE1.4-Ur-16	-91.0
PFE1.4-UU-20	-87.5

3.4. Small Angle X-ray Scattering (SAXS) studies

The SAXS intensity profiles of polyether, PDMS and PFE based copolymers are presented in Figure 3.15., Figure 3.16., and Figure 3.17. respectively. The positions of the interference peak in the intensity profiles are used to estimate the average interdomain spacing arising due to a periodic structure within the sample. The interdomain spacing is called Bragg or *d* spacing. The following formula is used to calculate the interdomain spacing: $d = (2\pi)/q_{max}$, where $q=(4\pi/\lambda)\sin\theta$, and 2θ equals radial scattering angle. The calculated values of interdomain spacing's are given in Table 3.4. The copolymers that are not presented in Table3.4., either did not have mechanical integrity to get SAXS measurements, measurements were taken but no peak was obtained or a peak was obtained but it was not well defined so did not allowed *d* calculations. For some of these mentioned copolymers observation of well-defined SAXS peaks were reported in the literature [10, 30], however with the equipment we were using it was not possible to reproduce these data due to technical restrictions.

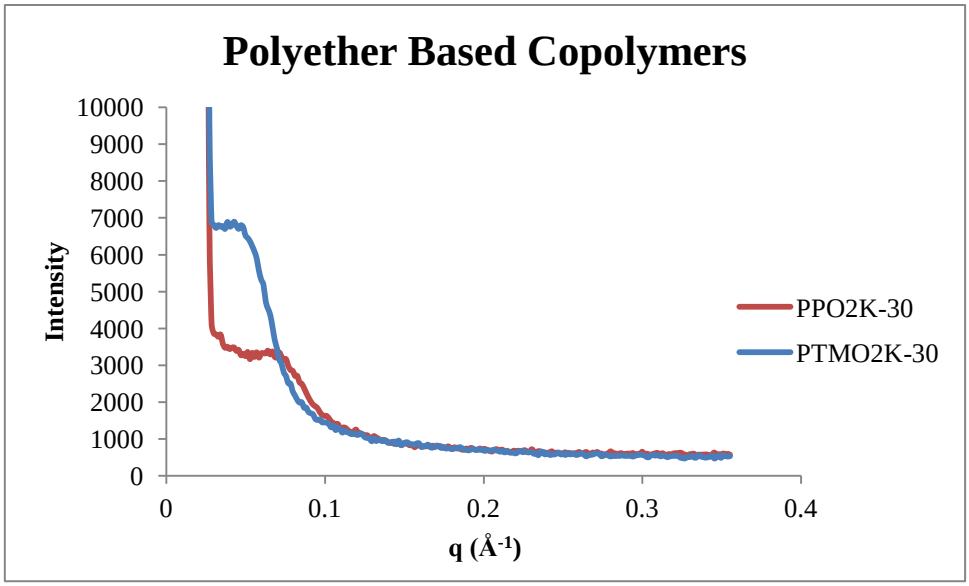

Figure3.15. SAXS intensity profiles of PPO2-UU-30 and PTMO2-UU-30.

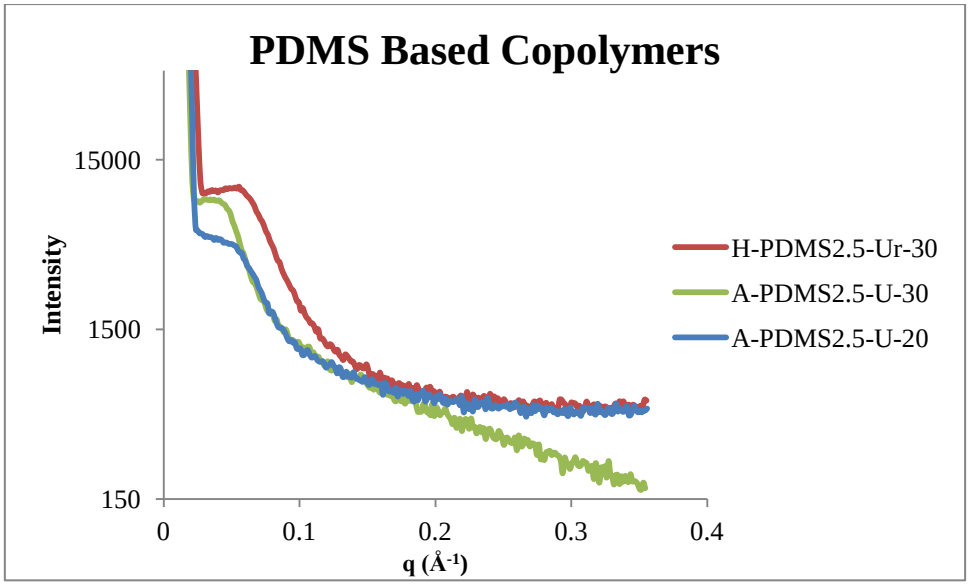

Figure 3.16. SAXS intensity profiles of H-PDMS2.5-Ur-30, H-PDMS2.5-Ur-30 and A-PDMS2.5-U-30.

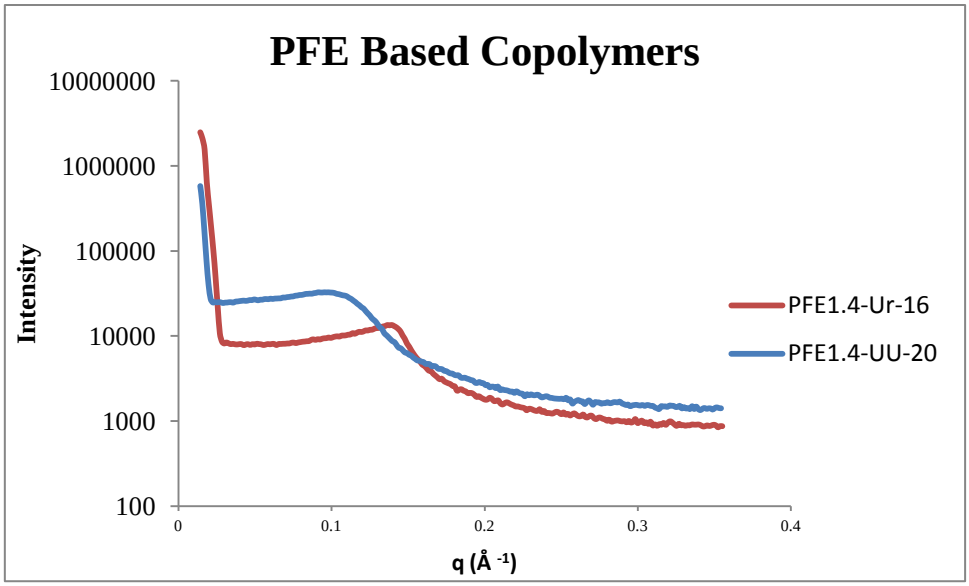

Figure 3.17. SAXS intensity profiles of PFE1.4-Ur-16 and PFE1.4-UU-20.

Table 3.3. Calculated interdomain spacings (*d*) of copolymers.

Sample Name	*d* (nm)
PPO2-UU-30	9.8
PTMO2-UU-30	14.7
H-PDMS2.5-Ur-30	11.3
A-PDMS2.5-U-20	13.3
A-PDMS2.5-U-30	18.9
PFE1.4-Ur-16	4.5
PFE1.4-UU-20	6.5

As can be seen from Table 3.3., when polyethers are compared with each other, PEO2-UU-30 does not show a SAXS peak and PPO2-UU-30 has a smaller *d* compared with PTMO2-UU-30. This is expected since *d* is expected to increase with better microphase separated structures and PEO has the highest solubility parameter (20.2 $(J/cm^3)^{1/2}$) when compared with PPO (18.9 $(J/cm^3)^{1/2}$) and PTMO (17.6 $(J/cm^3)^{1/2}$) which results in stronger interaction with the hard segments leading to phase mixing.

A-PDMS2.5-UU-30 has the largest *d* spacing which is also expected, since it has excellent microphase separation due to the polarity and solubility parameter differences between PDMS and urea groups. H-PDMS2.5-Ur-30 has a smaller *d* when compared with their urea homologs and H-PDMS2.5-Ur-20 did not show a peak. This suggests that microphase separation in PDMS based TPUs is somewhat poorer when compared with their urea counterparts. The formation of smaller HS domains in TPUs due to phase mixing and formation of a thick interphase/interface between continuous SS and dispersed HS is possible. It has also been demonstrated that somewhat excellent microphase separation in PDMS based TPUs with very sharp interface between microphases also influence their thermal and mechanical properties dramatically. [28] The solubility parameter of urethane being less than urea as well as diminished hydrogen bonding capacity of urethanes when compared with ureas were also suggested to influence the thermal and mechanical properties. The effect of HS content can also be observed with A-PDMS2.5-U-20 and A-PDMS2.5-U-30. As expected the 20% wt HS copolymer (13.3 nm) has a smaller interdomain spacing when compared with its 30% wt HS counterpart (18.9 nm).

It is interesting that PFE based copolymers have the smallest interdomain spacings. Other characterization techniques show that these polymers do have a microphase separated structure because of the very low the solubility parameter of E10-H® (<15 $(J/cm^3)^{1/2}$), which is even lower than that of PDMS (15.6 $(J/cm^3)^{1/2}$). This implies that the ordering of the HS in these copolymers, as well as their corresponding morphologies, is very different from the rest of the copolymers. Indeed a unique morphology was seen in the AFM pictures for these copolymers as provided on Figure 3.17. The reasons for such smaller values may be due to: (i) The molecular weight of E10-H® is smaller when compared with the other copolymers. (ii) Fluorine has the highest electronegativity among all elements and the second smallest atomic radius after hydrogen. In a carbon-fluorine bond, a carbon atom is being strongly attracted by the most electronegative fluorine therefore generating a very strong and short covalent bond. The fluorine atom covers the carbon atoms without spacing therefore fluoropolymers are expected to have stiff spatial structures. [33, 68] The effect of HS content can also be observed in these copolymers. As expected the 16% by wt HS TPU analogs have smaller interdomain spacings (4.5 nm) when compared with 20%wt HS PUU analogs (6.5 nm).

3.5. Stress-Strain Analysis

When comparing polyether based copolymers, it is seen that PTMO2-PUU-30 shows the highest tensile strength and modulus among all copolymers (Table 3.4.). PTMO has the lowest solubility parameter when compared with PEO and PPO and therefore it is expected to have the highest extent of microphase separation among polyethers as has also been observed in the SAXS experiments. This explains why PTMO1-PU-30 copolymers have mechanical integrities at RT while their PEO and PPO analogs are too soft to form films at RT. As molecular weights of the oligomers are increased to 2K g/mol, copolymers containing 20% HS with PPO SS show very weak properties and copolymers containing PEO SS do not form a film at RT due to extensive phase mixing. Polymers containing 30% HS with PEO and PPO SS form films with good mechanical integrity, however with lower tensile strengths when compared to their PTMO analogs. From ATR-FTIR characterizations we know that PEO2-PUU-30 has urethane linkages free from hydrogen bonding in their structure, also this copolymer did not show any peak in SAXS measurements indicating phase mixing. Even though there is reasonably high extent of phase mixing in PEO2-PUU-30, it still displays very good mechanical properties with an ultimate tensile strength of 20 MPa. However, its elongation at break value of 260% is somewhat lower than expected for such elastomers, most probably due to the crystallinity of PEO segments. The mechanical properties of PEO based copolymers are due to the ability of PEO to crystallize and go through strain induce crystallization when they are above a certain molecular weight as was confirmed with DSC measurements. Crystallites are thought to act as additional load bearing units, which are capable of absorbing strain energy. Indeed, this behavior has been characterized in the literature before. Korley et. al. tuned the crystallinity of the PEO SS and characterized these copolymers. They found that introducing crystallizable PEO units enhanced toughness and extensibility of TPUs compared to their amorphous analogs with the same HS contents.[9]

All PDMS based PU have very high modulus values and therefore have very low elastic properties as expected. The excellent microphase separation of the HS and the bidentate nature of the urea linkages, allow these HS to act as perfect fillers and therefore makes them very rigid in nature. Increased SS $<M_n>$ in these copolymers leads to better elastic properties since it allows increased mobility in the copolymer. However it is interesting to observe that PTMO2-PUU-30 has much higher TS than PDMS copolymers even though the PDMS oligomers have an average molecular weight of 2.5K g/mole, have better microphase separation and consist of pure urea linkages while PTMO based copolymers consist of

urethane/urea linkages. This can be explained with PTMO's ability to strain-crystallize during mechanical tests. When PTMO segments are longer than 1K g/mol, they are able to strain crystallized at high strain rates thereby strain hardening the copolymer at RT [29]. As discussed above, the crystals can act as load bearing units.

Table 3.4. Tensile properties of copolymers.

Copolymer Designation	**Modulus(MPa)**	**Tensile Strenght (MPa)**	**Elongation(%)**
PEO1-UU-30	very soft	very soft	very soft
PEO2-UU-20	brittle	brittle	brittle
PEO2-UU-30	5.0	20.0	260
PPO1-UU-30	very soft	very soft	very soft
PPO2-UU-20	1.4	5.0	>1000
PPO2-UU-30	7.0	25.0	940
PTMO1-UU-25	3.0	10.0	900
PTMO1-UU-30	5.0	12.0	670
PTMO2-UU-20	5.0	30.0	780
PTMO2-UU-30	20.0	40.0	670
H-PDMS1-Ur-30	25.0	5.3	400
H-PDMS2.5-Ur-30	20.0	5.0	220
A-PDMS1-U-22.5	180.0	20.0	430
A-PDMS1-U-30	brittle	brittle	brittle
A-PDMS2.5-U-20	20.0	10.0	200
A-PDMS2.5-U-30	30.0	10.0	80
PFE1.4-UU-20	40.0	5.0	30

When comparing PDMS based copolymers the dramatic effect of the bidentate nature of the hydrogen bonding between urea groups versus the monodentate hydrogen bonding between urethane groups can clearly be observed. The copolymers with urea links show much higher modulus and tensile strength values when compared with their urethane analogs. This concept has also been described in literature before [14].

The PFE based copolymers show very good mechanical properties taken into account that their low molecular weight of E10H® and their low HS content. Similar to their PDMS based analogs, PFE1.4-PUU-20 has excellent microphase separation therefore has high modulus values and low elongation %. They are hard to compare with PDMS based copolymers since they have both urea and urethane linkages and they are hard to compare with polyether based copolymers since their molecular weight is in between the varying molecular weights for these copolymers.

3.6. Surface Characterization

3.6.1 Atomic Force Microscopy

The nano structures of STPEs including TPUs, PUUs and PUs, have long been characterized in the literature by using AFM. [69] AFM presents real space visual characterization of the organization, dimension, shape and dispersion of the HS domains in microphase separated structures of copolymers. In the literature, phase images of microphase separated structures are reported to be globular, fibrillar or ribbon like depending how well microphase separation has occurred. [14, 69] Well defined fibrillar microphase separated structures of *non chain extended* PTMO1K/HMDI PU can be observed in Figure 3.18. The lighter regions in the phase image correspond to HS.

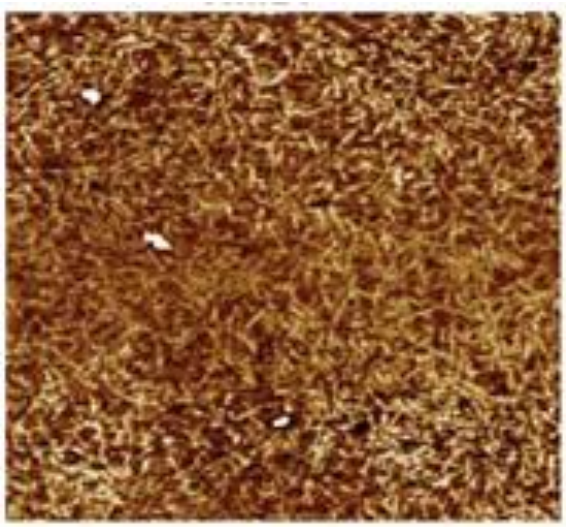

Figure3.18. AFM phase image of *non chain extended* PTO1K/HMDI PU. [14]

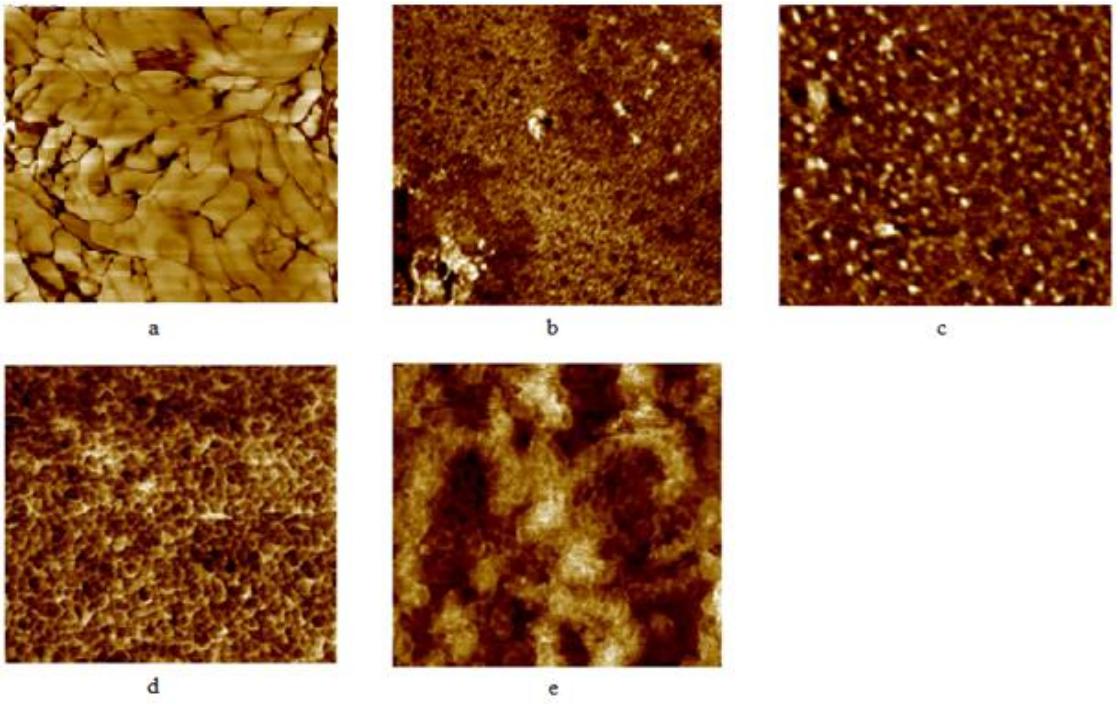

Figure 3.19. AFM phase images of copolymers. a)PEO2-UU-30 b)PPO2-UU-30 c)PTMO2-UU-30 d)A-PDMS2.5-U-30 e)PFE1.4-UU-20. (PTMO and PPO based copolymer pictures are 1µm X 1µm in size, PEO based copolymer picture is 2µm X 2µm and PDMS and PFE based copolymer pictures are 0.5 µm X 0.5 µm size)

AFM phase images for the copolymers synthesized are provided in Figure 3.19 (a-e). As can be seen in Figure 3.19. (a), PEO2-UU-30 shows the presence of crystalline PEO on the film surface. It is interesting to observe that the urea linked *non-chain extended* PTMO1K/HMDI (Figure 3.18.) shows well defined fibrillar like microphase separated structures while PTMO2-UU-30 (Figure 3.19. (c)) shows a globular and less microphase separated structure. The bidentate nature of the urea linkages enables the HS to separate from the SS while the monodentate nature of urethane linkages is not strong enough to facilitate this separation to a well defined extent. This form of microphase separation in PTMO2K with HS consisting of HMDI has been reported in the literature previously as can be seen in Figure 3.20. [69] So in comparison, PTMO2K-PUU-30 is the only polyether based copolymer that gives a well defined AFM image indicating a microphase separated morphology.

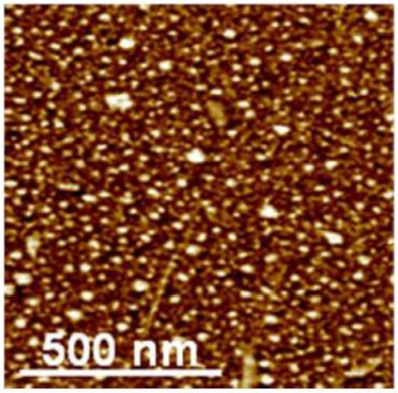

Figure 3.20. AFM phase image of PTMO2K/HMDI/DETA, 28%wt HS. [69]

The absence of fibrillar or ribbon like bright regions in the AFM images of the polyether based segmented copolymers generally indicate phase mixing in these copolymers. This is expected since the solubility parameters of polyethers are close to urea and urethanes and HMDI-MDAP are unsymmetrical HS, making it hard for them to pack. Especially PEO and PPO based copolymers shows no indication of microphase separation in their surface morphology.

PFE1.4-UU-20 shows an interesting surface morphology. As expected and was also confirmed by XPS results, the surface is mostly covered with the SS, due to its fairly low surface energy, therefore the structure we see is not a representation of the microphase separation in the bulk polymer.

In a study conducted by Yilgor et.al. the surface of the silicone-urea copolymers were modeled by using molecular dynamics (MD) and mesoscale dynamic simulations. [31] Amine terminated PDMS oligomers with varying average molecular weights were used as the SS and HMDI was used as the HS. Figure 3.21. represents a model of a *non-chain extended* copolymer based on A-PDMS with an average molecular weight of 3,200 g/mol. The data presented in this thesis provides complimentary information on the model demonstrated by Yilgor et. al. The color distribution looks homogenous, therefore the globular domains resemble silicones that have migrated on the surface as was proposed by Yilgor et.al. by using molecular dynamic and mesoscale dynamic simulations. The XPS and static water contact angle data also supports the surface being composed of silicone.

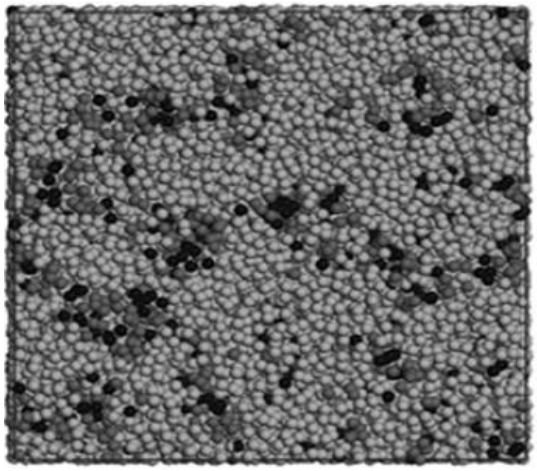

Figure 3.21. Microphase morphology of A-PDMS3K/HMDI, 8% by wt HS obtained by bead representation using Dissipative Particle Dynamics calculations. PDMS segments are shown in gray, urea HS in dark gray and HMDI methyl groups in black in color. [31]

3.7. X-ray Photoelectron Spectrometry (XPS)

In order to better understand the surface compositions of the copolymers, which are almost always different than that of bulk, atomic compositions of the SS oligomers, the diisocyanate (HMDI) and the chain extender (MDAP) are provided as follows: PEO: (2 Carbon + 1 Oxygen); PPO: (3 Carbon + 1 Oxygen); PTMO: (4 Carbon + 1 Oxygen); PDMS: (2 Carbon + 1 Oxygen + 1 Silicone); PFE: (7 Carbon + 4 Oxygen + 6 Fluor). HMDI: (16 Carbon + 2 Oxygen + 2 Nitrogen); MDAP: (5 Carbons, 2 Nitrogen). Since XPS gives percent atomic composition of the surfaces Table 3.5 provides the percent atomic compositions of the starting materials.

Table 3.5. Percent Atomic Composition of the Starting Materials used during the preparation of TPUU copolymers

	Atomic % Composition				
Sample	**Carbon**	**Oxygen**	**Nitrogen**	**Silicone**	**Fluor**
PEO	66.7	33.3	-	-	-
PPO	75	25	-	-	-
PTMO	80	20	-	-	-
PDMS	50	25	-	25	-
PFE	41.2	23.5	-	-	35.3
HMDI	80	10	10	-	-
MDAP	71.4	-	38.6	-	-

In order to better analyze the XPS results obtained, bulk atomic compositions of the copolymers are provided on Table 3.6.

A summary of the XPS data obtained on all copolymers synthesized in this study are presented in Table 3.7.

Table 3.6. Percent Bulk Atomic Compositions of the Copolymers (calculated from the reaction stoichiometry)

	Bulk Atomic Compositions (calculated)				
Sample	**Carbon**	**Oxygen**	**Nitrogen**	**Silicone**	**Fluor**
PEO2-UU-20	78.0	10.7	11.3	-	-
PEO2-UU-30	78.0	9.4	12.6	-	-
	% Atomic Composition				
Sample	**Carbon**	**Oxygen**	**Nitrogen**	**Silicone**	**Fluor**
PPO2-UU-30	78.25	9.15	12.6	-	-
	% Atomic Composition				
Sample	**Carbon**	**Oxygen**	**Nitrogen**	**Silicone**	**Fluor**
PTMO1-UU-30	79.25	10.5	10.25	-	-
PTMO2-UU-20	79.1	10.15	10.75	-	-
PTMO2-UU-30	78.63	9.16	12.21	-	-
	% Atomic Composition				
Sample	**Carbon**	**Oxygen**	**Nitrogen**	**Silicone**	**Fluor**
A-PDMS1-U-30	75.75	11.11	10.1	3.04	-
A-PDMS2.5-U-20	76.25	9.65	12.1	2.0	-
A-PDMS2.5-U-30	76.95	8.92	12.89	1.24	-
	% Atomic Composition				
Sample	**Carbon**	**Oxygen**	**Nitrogen**	**Silicone**	**Fluor**
PFE1.4-UU-20	64.4	14.96	6.74	-	13.9

Table 3.7. Percent Atomic Compositions of Copolymers obtained from XPS analyses

	Atomic % Composition by XPS				
Sample	**Carbon**	**Oxygen**	**Nitrogen**	**Silicone**	**Fluor**
PEO2-UU-20	70	28	2	-	-
PEO2-UU-30	73	25	2	-	-
	Atomic % Composition				
Sample	**Carbon**	**Oxygen**	**Nitrogen**	**Silicone**	**Fluor**
PPO2-UU-30	77	20	3	-	-
	Atomic % Composition				
Sample	**Carbon**	**Oxygen**	**Nitrogen**	**Silicone**	**Fluor**
PTMO1-UU-30	70	28	2	-	-
PTMO2-UU-20	79	18	3	-	-
PTMO2-UU-30	79	18	3	-	-
	Atomic % Composition				
Sample	**Carbon**	**Oxygen**	**Nitrogen**	**Silicone**	**Fluor**
A-PDMS1-U-30	60	18	5	17	-
A-PDMS2.5-20	55	20	2	23	-
A-PDMS2.5-30	55	20	3	22	-
	Atomic % Composition				
Sample	**Carbon**	**Oxygen**	**Nitrogen**	**Silicone**	**Fluor**
PFE1.4-UU-20	40	17	2	-	42

Considering some carbon impurities exist for every sample, polyether based copolymers show a close trend to the ratio of their SS. Also when they are compared with their bulk compositions, the high percentage of oxygen and low percentage of nitrogen draws our attention thus we can say that the surfaces are mostly covered with SS. However they are not completely covered since we see trace amounts of nitrogen.

Considering some carbon impurities exists, especially the PDMS based copolymers based on 2.5K oligomers show a very close trend to the ratio of their SS compositions rather than their bulk compositions, thus we can say that the surfaces are dominantly covered with SS. The migration of PDMS towards the surface to lower the materials surface energy is favored therefore this result was expected. However it is interesting to observe that the PDMS1-U-30 has carbon to oxygen ratios not compliant with its SS carbon to oxygen ratios. The excess amount of nitrogen and carbon compared with the other samples gives an idea that the surface is less covered with SS for PDMS1-U-30.

The PFE based copolymer shows a higher amount of Fluor atoms than expected indicating the surface is dominantly composed of E10-H® SS. This is also an expected result since E10-H® will reduce surface energy.

3.8. Static Water Contact Angle Measurements

Static water contract angles of representative copolymers based on PEO, PPO, PTMO, PDMS and PFE are provided on Table 3.8. together with the surface tension values of the pure soft segment oligomers. As can be seen on Table 3.20. PDMS and PFE based copolymers have very high contact angles around 110° clearly demonstrating surfaces are covered by low energy SS and therefore are highly hydrophobic (>90˚), which is expected. On the other hand static water contact angles of polyether based copolymers are lower than 90˚ making them somewhat hydrophilic.

It is interesting to note that PPO and PTMO based copolymers display almost similar water contact angles of around 80°, whereas highly hydrophilic PEO based copolymer displays a much lower contact angle around 30°. These are all expected results as will be explained below. The contact angles of copolymers with differing hard segments or molecular weight were found to be very similar to these results.

Table 3.8. Average static water contact angles measured on PUU copolymers

Sample Name	Average Water Contact Angles
PEO2K-30	28.0˚±1.4˚
PPO2K-30	78.7˚±0.9˚
PTMO2K-30	79.5˚±0.3˚
A-PDMS2.5K-30	110.0˚±0.9˚
PFE1.6K-20	106.2˚±1.2˚

The differences in the static water contact angles on various surfaces can be rationalized as follows: Water has a relatively high surface tension value of 73 mJ/m^2. The hydrogen bonding forces are mainly responsible for this high surface tension (intermolecular forces) of water. Extremely low surface tension values of PFE (20 mJ/m^2) and PDMS (21 mJ/m^2) based polymers are mainly caused by the weak dispersion forces. Therefore very little

intermolecular interaction is possible across a water/fluorocarbon or water/silicone interface which results in a large interfacial tension and thus high contact angle. In contrast, polyether based copolymers, depending on the polyether structure, have a tendency towards hydrogen bonding with water through ether linkages and therefore result in higher water contact angle values. “Unlike materials” will seek to minimize free energy in the interfacial region therefore minimize the interfacial area (large contact angles) whereas “like molecules” (similar intermolecular forces) will have no interfacial tension (small contact angles). [68] PEO has the highest solubility parameter and highest frequency of oxygen in its structure enabling an increased interaction with water making it super hydrophilic.

Water contact angle results provide strong confirmation to the data obtained by XPS. We had predicted that the surfaces are mostly covered with SS from XPS, and from water contact angles measurements can see that the surface properties are mostly determined by the SS structure.

3.9. Biofilm Assays

Medical grade PVC was used as the control polymer of these experiments. *Staphylococcus aureus* 700698 strain bacterium was used in the experiments because this strain is well known to form mature biofilms very easily. These biofilms are the cause pneumonia in patients that use endotracheal tubes for breathing after surgery. Different polymers were tested in order to study the correlation of polymer surface energy to the attachment of the bacterium. The results of these biofilm assays are presented in Table 3.9. A minimum of a three log decrease in the colony counts is considered as a significant result indicating inhibition of biofilm growth.

There have been various suggestions in the literature on the sticking mechanism of bacterium to surfaces. [2, 3] However it is very hard to pin down the exact cause of sticking at this point. This problem needs to be approached from different angles to characterize the sticking mechanism of bacterium on surfaces. Thus we tried varying the surface energies of the copolymers and experimented if there would be a reduction on the biofilm formation. As seen from the results, all samples were capable of forming mature biofilms. It was concluded that considering the segmented TPUU prepared and tested in this study, the surface composition

or the surface energy energy did not seem to play a significant role for the inhibition of biofilm formation on the polymer surfaces by *Staphylococcus* aureus 700698.

Table 3.9. The colony counts of polymers with varying surface energies. (It should be noted that SLM TPSE-140 is a commercial two phase block copolymer containing PDMS as its soft segment and an aliphatic isocyanate as its hard segment. It contains more than 90% by wt of dimethylsiloxane.)

	Sample Name	**Colony Count (cfu)**
Batch1	Medical grade PVC	1.95×10^6
	SLM TPSE-140	2.81×10^6
Batch2	Medical grade PVC	4.54×10^6
	PTMO2-UU-20	3.26×10^5
Batch 3	Medical grade PVC	2.53×10^5
	PFE1.6-UU-20	4.33×10^5

CHAPTER 4

CONCLUSIONS

A large number of segmented thermoplastic TPUUs, TPUs and PUs based on five different SS with varying SS <Mw> and HS content were successfully synthesized and characterized. Effect of the SS structure, SS <Mw> and HS content on the bulk and surface properties were studied. Also the correlation between the surface energy of the copolymers with the biofilm formation was studied.

Characterization results showed that polyether based copolymers, especially those with PEO SS, displayed poor microphase separation when compared with PDMS and PFE based copolymers.

The carbonyl regions in the ATR-FTIR spectra revealed that the polyether based copolymers had significant phase mixing between the urea/urethane groups in the HS and the ether oxygens present in the SS structure. The urethane groups of the polyether based copolymers showed peaks in the weakly hydrogen bonded regions and urea groups had peaks in the free urea region as well as the ordered hydrogen bonded region. PEO2-PUU-20 had even a shoulder of peak in the free urethane region indicating an excessive amount of phase mixing. When comparing all PUUs, only PDMS and PFE based polymers show medium to strong hydrogen bonded urethane groups around 1695 cm^{-1}. PDMS based TPUs start showing shoulders at 1663 cm^{-1} indicating very strongly bonded urethane groups, when their <Mw> is increased from 900 g/mol to 2.500 g/mol.

Other bulk characterizations consist of DSC, SAXS and stress-strain tests. DSC measurements confirmed that all samples had microphase separated morphologies. To better analyze the extent of these separations, SAXS measurements were done. As expected, the interdomain spacing increased with increased microphase separation except for PFE based copolymers. This implied that the ordering of the HS in these copolymers, as well as their corresponding morphologies, is very different from the rest of the copolymers. Stress-strain tests showed us that the modulus of the samples increased with increased microphase separation, whereas tensile strength values depended on strain induce crystallization as well as microphase separated morphology.

Surface characterizations consisted of AFM, XPS and static water contact angle measurements. Among the polyether based copolymers, only PTMO2-UU-30 showed a somewhat microphase separated morphology. PDMS based copolymers gave a picture largely consisting of silicones and PFE based copolymers showed a unique structure. Surface characterization by contact angle measurements showed dramatic differences depending on the SS structure and molecular weight. As indicated by XPS studies, in general the soft segments tend to migrate to the polymer surface and affect the hydrophobicity and hydrophilicity of the copolymer depending on their solubility parameters.

Biofilm assays on copolymers having different surface energies were conducted. Results showed that all samples were capable of forming mature biofilms. It was concluded that the surface energies did not play a role for *Staphylococcus* aureus 700698 to form biofilms.

BIBLIOGRAPHY

1. Khil Myung-Seob, C.D.-I., Kim Hak-Yong, Kim In-Shik, Bhattarai Narayan *Electrospun Nanofibrous Polyurethane Membrane as Wound Dressing.* Biomedical Materials Research 2003. **67**: p. 675-679.
2. Bazaka, K., et al., *Plasma-assisted surface modification of organic biopolymers to prevent bacterial attachment.* Acta Biomaterialia, 2011. **7**(5): p. 2015-2028.
3. Yao, X., Y.L. Song, and L. Jiang, *Applications of Bio-Inspired Special Wettable Surfaces.* Advanced Materials, 2011. **23**(6): p. 719-734.
4. Bazaka, K., et al., *Efficient surface modification of biomaterial to prevent biofilm formation and the attachment of microorganisms.* Applied Microbiology and Biotechnology, 2012. **95**(2): p. 299-311.
5. William, J.B., *The Origin of the Polymer Concept* Journal of Chemical Education 2008(85): p. 624-625.
6. Priscila, A., *Nanocomposites - New Trends and Developments*, ed. E. Farzad. 2012.
7. Odian, G., *Principles of Polymerization* 4ed. 2004, USA: JOHN WILEY & SONS, INC.
8. Klinedinst, D.B., et al., *The effect of varying soft and hard segment length on the structure-property relationships of segmented polyurethanes based on a linear symmetric diisocyanate, 1,4-butanediol and PTMO soft segments.* Polymer, 2012. **53**(23): p. 5358-5366.
9. Korley, L.T.J., et al., *Effect of the degree of soft and hard segment ordering on the morphology and mechanical behavior of semicrystalline segmented polyurethanes.* Polymer, 2006. **47**(9): p. 3073-3082.
10. Ertem, S.P., et al., *Effect of soft segment molecular weight on tensile properties of poly(propylene oxide) based polyurethaneureas.* Polymer, 2012. **53**(21): p. 4614-4622.
11. Yilgor Emel, Y.I., *Silicone containing copolymers: Synthesis, properties and applications.* Progress in Polymer Science 2013(848).
12. Bil, M., et al., *Optimization of the structure of polyurethanes for bone tissue engineering applications.* Acta Biomaterialia, 2010. **6**(7): p. 2501-2510.
13. Yilgor, I., et al., *FTIR investigation of the influence of diisocyanate symmetry on the morphology development in model segmented polyurethanes.* Polymer, 2006. **47**(11): p. 4105-4114.
14. Yilgor Iskender, Y.I., *Structure-Morphology-Property Behavior of Segmented Thermoplastic Polyurethanes and Polyureas Prepared without Chain Extenders.* Polymer Reviews, 2007. **47**: p. 487-510.
15. Kanyanta, V. and A. Ivankovic, *Mechanical characterisation of polyurethane elastomer for biomedical applications.* Journal of the Mechanical Behavior of Biomedical Materials, 2010. **3**(1): p. 51-62.
16. Otto, B., *Das Di-Isocyanat-Polyadditionsverfahren(Polyurethane).* Angewandte Chemie, 1947. **59**(9): p. 257-272.
17. Schollenberger, S.C., *Simulated vulcanizates of polyurethane elastomers*. 1959, Google Patents.
18. Cooper S.L., T.A.V., *Properties of linear elastomeric polyurethanes.* Journal of Applied Polymer Science, 1966. **10**(12): p. 1837-1844.
19. Stoyko, F., *Handbook of Condensation Thermoplastic Elastomers*. 2005: WILEY-VCH.
20. Yilgor, I., et al., *Contribution of soft segment entanglement on the tensile properties of silicone-urea copolymers with low hard segment contents.* Polymer, 2009. **50**(19): p. 4432-4437.
21. Campbell, I.M., *Introduction to Synthetic Polymers*. 1994, USA: Oxford University Press Inc. .
22. Yilgor, E., et al., *Comparison of hydrogen bonding in polydimethylsiloxane and polyether based urethane and urea copolymers.* Polymer, 2000. **41**(3): p. 849-857.

23. Yilgor, E., I. Yilgor, and E. Yurtsever, *Hydrogen bonding and polyurethane morphology. I. Quantum mechanical calculations of hydrogen bond energies and vibrational spectroscopy of model compounds.* Polymer, 2002. **43**(24): p. 6551-6559.
24. Yilgor, E., E. Yurtsever, and I. Yilgor, *Hydrogen bonding and polyurethane morphology. II. Spectroscopic, thermal and crystallization behavior of polyether blends with 1,3-dimethylurea and a model urethane compound.* Polymer, 2002. **43**(24): p. 6561-6568.
25. Das Sudipto , C.D.F., Wilkes Garth L., Klinedinst Derek B., Yilgor Iskender, Yilgor Emel, Beyer Frederick L. , *Effect of Symmetry and H-bond Strength of Hard Segments on the Structure-Property Relationships of Segmented, Nonchain Extended Polyurethanes and Polyureas.* Macromolecular Science, Part B: Physics, 2007. **46**(5): p. 853-875.
26. E.A., G., *Polymer Handbook*, ed. I.E.H. Brandrup J. 1989: WILEY. 519-559.
27. Patrick, R.L., *Treatise on Adhesion and Adhesives*. Vol. 5. 1981, USA: Marcel Dekker.
28. Yilgor, E. and I. Yilgor, *Hydrogen bonding: a critical parameter in designing silicone copolymers.* Polymer, 2001. **42**(19): p. 7953-7959.
29. Biemond, G.J.E. and R.J. Gaymans, *Elastic properties of thermoplastic elastomers based on poly(tetramethylene oxide) and monodisperse amide segments.* Journal of Materials Science, 2010. **45**(1): p. 158-167.
30. Sheth, J.P., et al., *Influence of system variables on the morphological and dynamic mechanical behavior of polydimethylsiloxane based segmented polyurethane and polyurea copolymers: a comparative perspective.* Polymer, 2004. **45**(20): p. 6919-6932.
31. Yildirim, E., et al., *Multiscale Modeling of the Morphology and Properties of Segmented Silicone-Urea Copolymers.* Journal of Inorganic and Organometallic Polymers and Materials, 2012. **22**(3): p. 604-616.
32. John, S., *Structure/Property Considerations for Fluoropolymers and Fluoroelastomers to Avoid In-service Failure*. Modern Fluoropolymers: High Performance Polymers for Diverse Applications ed. S. John. 1997: John Wiley & Sons Ltd. .
33. JunkoshaInc. *The Features of Fluoropolymers* 02.06.2014]; Available from: http://www.junkosha.co.jp/english/hyper/hyper_ex.html.
34. Pozzoli M., V.G., Arcella V., *Melt-processable Perfluoropolymers*. Modern Fluoropolymers, ed. J. Scheirs. 1997: John Wiley & Sons.
35. Brady Robert F., J., *Fluorinated Polyurethanes*. Modern Fluoropolymers: High Performance Polymers for Diverse Applications ed. J. Scheirs. 1997: John Wiley & Sons Ltd.
36. O'Sickey Matthew J., L.B.D., Wilkes Garth L., *Structure–Property Relationships of Poly(urethane urea)s with Ultra-low Monol Content Poly(propylene glycol) Soft Segments. I. Influence of Soft Segment Molecular Weight and Hard Segment Content.* Journal of Applied Polymer Science, 2002. **84**: p. 229-243.
37. Velankar, S. and S.L. Cooper, *Microphase separation and rheological properties of polyurethane melts. 1. Effect of block length.* Macromolecules, 1998. **31**(26): p. 9181-9192.
38. Van der Schuur, M. and R.J. Gaymans, *Segmented block copolymers based on poly(propylene oxide) and monodisperse polyamide-6,T segments.* Journal of Polymer Science Part a-Polymer Chemistry, 2006. **44**(16): p. 4769-4781.
39. Sarva, S.S. and A.J. Hsieh, *The effect of microstructure on the rate-dependent stress-strain behavior of poly(urethane urea) elastomers.* Polymer, 2009. **50**(13): p. 3007-3015.
40. Hernandez, R., et al., *A Comparison of Phase Organization of Model Segmented Polyurethanes with Different Intersegment Compatibilities.* Macromolecules, 2008. **41**(24): p. 9767-9776.
41. Leung L.M., K.J.T., *Small-angle scattering analysis of hard-microdomain structure and microphase mixing in polyurethane elastomers.* Journal of Polymer Science: Polymer Physics Edition, 1985. **23**(9): p. 1883-1913.
42. Saiani, A., et al., *Origin of multiple melting endotherms in a high hard block content polyurethane. 2. Structural investigation.* Macromolecules, 2004. **37**(4): p. 1411-1421.

43. Barikani M, H.C., *The relative thermal stability of polyurethane elastomers: Influence of chain extender structure.* Cellular Polymers, 1987. **6**: p. 47-67.
44. Yilgor, I., et al., *Time-Dependent Morphology Development in Segmented Polyetherurea Copolymers Based on Aromatic Diisocyanates.* Journal of Polymer Science Part B-Polymer Physics, 2009. **47**(5): p. 471-483.
45. Gaymans, R.J.F., Jan; Biemond, G.J.E., *Segmented Block Copolymers with Monodisperse Hard Segments: The Influence of H-Bonding on Various Properties.* Macromolecular Materials and Engineering, 2009. **294**(8): p. 492-502.
46. J, Z., *Encyclopedia of Polymer Science and Technology*. Polyamides. Vol. 11. 1964, NewYork: Wiley
47. Wittbecker E. L., H.R.C., Watkins W. W. , *Elastic N-Substituted Polyamides.* Industrial&Engineering Chemistry, 1948. **40**(5): p. 875-879.
48. RJW, L.J.R., *N-Substitution in Polyamides.* Chemistry and Industry, 1951. **10**: p. 958-961.
49. Boretos J.W., P.W.S., *Segmented polyurethane: a new elastomer for biomedical applications.* Science, 1967. **158**: p. 1481-1482.
50. Rosler, A., G.W.M. Vandermeulen, and H.A. Klok, *Advanced drug delivery devices via self-assembly of amphiphilic block copolymers.* Advanced Drug Delivery Reviews, 2012. **64**: p. 270-279.
51. Santerre, J.P., et al., *Understanding the biodegradation of polyurethanes: From classical implants to tissue engineering materials.* Biomaterials, 2005. **26**(35): p. 7457-7470.
52. Zhou Xuefeng, Z.T., Guo Dawei, Ning Gu, *A facile preparation of poly(ethylene oxide)-modified medicalpolyurethane to improve hemocompatibility.* Colloids and Surfaces A: Physicochemical and Engineering Aspects, 2014. **441**: p. 34-42.
53. Tang, Y.W., R.S. Labow, and J.P. Santerre, *Enzyme-induced biodegradation of polycarbonate polyurethanes: Dependence on hard-segment concentration.* Journal of Biomedical Materials Research, 2001. **56**(4): p. 516-528.
54. Tang, Y.W., et al., *Use of surface-modifying macromolecules to enhance the biostability of segmented polyurethanes.* Journal of Biomedical Materials Research, 1997. **35**(3): p. 371-381.
55. Balazs, D.J., et al., *Surface modification of PVC endotracheal tubes by oxygen glow discharge to reduce bacterial adhesion.* Surface and Interface Analysis, 2003. **35**(3): p. 301-309.
56. Triandafillu, K., et al., *Adhesion of Pseudomonas aeruginosa strains to untreated and oxygen-plasma treated poly(vinyl chloride) (PVC) from endotracheal intubation devices.* Biomaterials, 2003. **24**(8): p. 1507-1518.
57. Sottile, F.D., et al., *Nosocomial Pulmonary Infection - Possible Etiologic Significance of Bacterial Adhesion to Endotracheal-Tubes.* Critical Care Medicine, 1986. **14**(4): p. 265-270.
58. Balazs, D.J., et al., *Inhibition of bacterial adhesion on PVC endotracheal tubes by RF-oxygen glow discharge, sodium hydroxide and silver nitrate treatments.* Biomaterials, 2004. **25**(11): p. 2139-2151.
59. Rello, J., et al., *Reduced burden of bacterial airway colonization with a novel silver-coated endotracheal tube in a randomized multiple-center feasibility study.* Critical Care Medicine, 2006. **34**(11): p. 2766-2772.
60. Khil, M.S., et al., *Electrospun nanofibrous polyurethane membrane as wound dressing.* Journal of Biomedical Materials Research Part B-Applied Biomaterials, 2003. **67B**(2): p. 675-679.
61. Delebecq Etienne, P.J.-P., Boutevin Bernard, Ganachaud François, *On the Versality of Urethane/Urea Bonds: Reversibility, Blocked Isocyanate, and Non-isocyanate Polyurethane* Chemical Reviews, 2013. **113**(1): p. 80-118.
62. Dusek, K., M. Spirkova, and I. Havlicek, *Network Formation of Polyurethanes Due to Side Reactions.* Macromolecules, 1990. **23**(6): p. 1774-1781.
63. Spirkova, M. and K. Dusek, *Extent of Side Reactions and Gelation of Polyether Polyurethanes.* Polymer Bulletin, 1989. **22**(2): p. 191-198.

64. Gray, J.L., et al., *Effect of Hydrogen Bonding on the Amide II Band of Model Disubstituted Urea Compounds.* Applied Spectroscopy, 2009. **63**(12): p. 1409-1413.
65. Coleman, M.M., et al., *HYDROGEN-BONDING IN POLYMERS .4. INFRARED TEMPERATURE STUDIES OF A SIMPLE POLYURETHANE.* Macromolecules, 1986. **19**(8): p. 2149-2157.
66. Yilgor, I. and E. Yilgor, *Hydrophilic polyurethaneurea membranes: influence of soft block composition on the water vapor permeation rates.* Polymer, 1999. **40**(20): p. 5575-5581.
67. S.D., G., *Kirk-Othmer Encyclopedia of Chemical Technology*. Polyethers, Propylene Oxide Polymers. 2000: John Wiley & Sons, Inc.
68. Hougham Gareth, C.P.E., Johns Ken, Davidson Theodore, *Fluoropolymers2:Properties*. Material Properties of Fluoropolymers, ed. T.R. Richard. 1996, USA: Kluwer Academic/Plenum Publisher.
69. Strawhecker, K.E., et al., *Influence of microstructure on micro-/nano-mechanical measurements of select model transparent poly(urethane urea) elastomers.* Polymer, 2013. **54**(2): p. 901-908.

VITA

Melis Peniç was born in Oxford, UK in 1989. She completed her high school education in Beşiktaş Atatürk Anadolu Highschool in 2004. She was then enrolled in a BS dual diploma program between Istanbul Technical University and Montana State University. In her senior year she started part time working in the Biofilm Engineering Center at MSU and carried on working full time on the same project for half a year after graduation. She then started her Master's Degree studies at Koc University in Fall 2012.